

TWO-SCALE ANALYSIS FOR MULTISCALE LANDAU-LIFSHITZ-GILBERT EQUATION: THEORY AND NUMERICAL METHODS*

XIAOFEI GUAN[†], HANG QI[†], AND ZHIWEI SUN[‡]

Abstract. This paper discusses the theory and numerical method of two-scale analysis for the multiscale Landau-Lifshitz-Gilbert equation in composite ferromagnetic materials. The novelty of this work can be summarized in three aspects: Firstly, the more realistic and complex model is considered, including the effects of the exchange field, anisotropy field, stray field, and external magnetic field. The explicit convergence orders in the H^1 norm between the classical solution and the two-scale solution are obtained. Secondly, we propose a robust numerical framework, which is employed in several comprehensive experiments to validate the convergence results for the Periodic and Neumann problems. Thirdly, we design an improved implicit numerical scheme to reduce the required number of iterations and relaxes the constraints on the time step size, which can significantly improve computational efficiency. Specifically, the projection and the expansion methods are given to overcome the inherent non-consistency in the initial data between the multiscale problem and homogenized problem.

Key words. multiscale Landau-Lifshitz-Gilbert equation, two-scale analysis, convergence order, improved implicit scheme

MSC codes. 35B27, 65N12, 78M40, 82D40

1. Introduction. The composite ferromagnetic materials are widely used in practical engineering, such as electric motors [16], sensors [23], and data storage devices [29], due to their ability to achieve physical and chemical properties difficult for homogeneous materials [25]. The state of composite ferromagnetic materials is defined by the magnetic moment $\mathbf{m}^\varepsilon \in S^2$, which is the sphere-valued vector field, and $\varepsilon \ll 1$ represents the spatial period of microstructure. Then, the dynamics of \mathbf{m}^ε are characterized by the multiscale Landau-Lifshitz-Gilbert (LLG) equation

$$(1.1) \quad \partial_t \mathbf{m}^\varepsilon - \alpha \mathbf{m}^\varepsilon \times \partial_t \mathbf{m}^\varepsilon = - (1 + \alpha^2) \mathbf{m}^\varepsilon \times \mathbf{h}_{\text{eff}}^\varepsilon(\mathbf{m}^\varepsilon).$$

Here, $\alpha > 0$ denotes the damping constant. $\mathbf{h}_{\text{eff}}^\varepsilon(\mathbf{m}^\varepsilon)$ is the effective field, which typically includes the exchange field, anisotropy field, stray field, and external magnetic field. To overcome the difficulties arising from strong degeneracy and nonconvex constraint $|\mathbf{m}| = 1$ of LLG equation without considering multiscale characteristics [18], extensive studies have been conducted on the well-posedness of LLG equation, and the solutions are proved to exist both in the weak sense [2, 6] and in the strong sense [28, 7, 14, 8, 12].

When delving into the multiscale LLG equation (1.1), additional difficulties in analysis and simulation arise from the singular perturbation induced by ε [13, 22]. To address these problems, one can apply multiscale method to find the approximate solution of (1.1)

*Submitted to the editors DATE.

Funding: The work was supported by the National Natural Science Foundation of China (No. 12271409), the Natural Science Foundation of Shanghai (No. 21ZR1465800), the Interdisciplinary Project in Ocean Research of Tongji University and the Fundamental Research Funds for the Central Universities.

[†]School of Mathematical Sciences, Tongji University, Shanghai, 200092, China (guanxf@tongji.edu.cn, qihang7750@gmail.com).

[‡]School of Mathematical Sciences, Soochow University, Suzhou, 215006, China (sunzhiwei1029@gmail.com).

$$(1.2) \quad \mathbf{m}^\varepsilon(\mathbf{x}) \approx \mathbf{m}_0(\mathbf{x}) + \varepsilon \boldsymbol{\chi}\left(\frac{\mathbf{x}}{\varepsilon}\right) \cdot \nabla \mathbf{m}_0(\mathbf{x}),$$

where \mathbf{m}_0 is the homogenized solution, describing the macro behavior of (1.1). $\boldsymbol{\chi}\left(\frac{\mathbf{x}}{\varepsilon}\right)$ is the ε -scale corrector, as given in (2.11). Then, heterogeneous multiscale methods (HMM) of multiscale LLG equation [31, 21] have been proposed, which can significantly reduce the computational costs. The works [11, 26, 1, 9] have proved the approximation (1.2) in the sense of two-scale convergence. Suppose only the exchange field is considered in (1.1), and the periodic boundary condition is posed. In this case, it has been proved that the convergence order $O(\varepsilon)$ of (1.2) holds in the $L^2(\Omega)$ sense, and remains uniformly bounded in the $H^1(\Omega)$ sense [20]. Subsequently, [10] considered the effect of both the exchange field and the stray field in $\mathbf{h}_{\text{eff}}^\varepsilon(\mathbf{m}^\varepsilon)$ under the Neumann boundary condition. An approximation error in the H^1 norm is derived by designing a second-order corrector which satisfies specific geometric constraints. Moreover, it was found that approximation (1.2) has a convergence deterioration under the Neumann boundary condition. To address this scenario, a more accurate approximation is chosen as

$$(1.3) \quad \mathbf{m}^\varepsilon(\mathbf{x}) \approx \mathbf{m}_0(\mathbf{x}) + (\boldsymbol{\Phi}^\varepsilon(\mathbf{x}) - \mathbf{x}) \cdot \nabla \mathbf{m}_0(\mathbf{x}),$$

where $\boldsymbol{\Phi}^\varepsilon$ is the Neumann corrector defined in (2.29).

In the theoretical part of this work, we extend the analysis in [10] to a more realistic model based on Landau and Lifshitz's original consideration [18]. Compared to the simplified model of (1.1) with only the exchange field, our model further considers the contribution of the anisotropy field, stray field, and external magnetic field in the effective field $\mathbf{h}_{\text{eff}}^\varepsilon(\mathbf{m}^\varepsilon)$ of (2.1). It is worth noting that we focus on the periodic boundary problem of (1.1) and the corresponding approximation error of (1.2). The main difficulties arise from the specific second-order corrector of our multiscale LLG equation. Applying a similar strategy in [10], the total consistency error is decomposed into two parts: the two-scale approximation error and the stray field error. Finally, we derive the approximation error of (1.2) in the H^1 norm. Additionally, a uniform $W^{1,6}$ estimate of (1.1) is deduced by the inner elliptic estimate and the compactness of the torus.

Although the convergence order of approximation (1.2)-(1.3) have been proved in [10], a gap exists in their numerical simulation. It is worth noting that the theoretical analysis usually relies on specific smoothness assumptions, such as:

- The periodic perturbation coefficients in $\mathbf{h}_{\text{eff}}^\varepsilon(\mathbf{m}^\varepsilon)$ being C^2 continuous.
- The boundary of the area Ω being $C^{1,1}$ continuous.
- The initial data being sufficiently smooth.

However, it is hard to handle the above assumptions in the numerical simulation. Several numerical methods have been used to solve the LLG equation [4, 32]. Specifically, we refer to the work [4], which provides an implicit finite element method with unconditional convergence. When delving into the simulation of the multiscale LLG equation, it becomes computational prohibitive and eventually infeasible to achieve adequate numerical resolution [30, 33]. Thus, we design an improved implicit numerical scheme inspired by [4], where a semi-implicit iteration approach is employed to solve the nonlinear system that results from implicit temporal discretization. In contrast to the implicit treatment in [4], the improved implicit approach significantly reduces the required number of iterations and relaxes the constraints on the time step size, as shown in Table 1. Merging the improved implicit scheme with the two-scale

method, a numerical framework is provided to deal with the multiscale LLG equation. It is worth noting that the initial data of the multiscale problem (1.1) and its homogenized problem exhibit inherent non-consistency. Therefore, we propose two viable methods, the projection method and the expansion method, to overcome this difference. Finally, the convergence orders of both the Periodic and Neumann problems of (1.1) with complicated effective field $\mathbf{h}_{\text{eff}}^\varepsilon(\mathbf{m}^\varepsilon)$ are successfully verified, which implies the robustness of our numerical framework.

This paper is organized as follows. In section 2, the homogenized model and correctors of multiscale LLG equation are derived by the two-scale method. Moreover, the boundary and initial setting of the (1.1), together with the numerical framework are given. In section 3, we present the convergence results of both the Periodic and Neumann problems under approximation (1.2)-(1.3). In section 4, numerical results are conducted to validate the error estimates presented in the previous section, which imply the effectiveness and robustness of the proposed framework. Finally, conclusions are given in section 5.

2. Two-scale analysis and numerical discretization. In this work, we consider the multiscale LLG equation (1.1), with the effective field $\mathbf{h}_{\text{eff}}^\varepsilon$

$$(2.1) \quad \mathbf{h}_{\text{eff}}^\varepsilon(\mathbf{m}^\varepsilon) = \text{div}(\mathbf{a}^\varepsilon \nabla \mathbf{m}^\varepsilon) - K^\varepsilon(\mathbf{m}^\varepsilon \cdot \mathbf{u})\mathbf{u} + M^\varepsilon \mathbf{h}_a + \mu^\varepsilon \mathbf{h}_d[M^\varepsilon \mathbf{m}^\varepsilon],$$

where $\mathbf{m}^\varepsilon : \Omega \rightarrow S^2$ is the magnetic moment, and $\Omega \subset \mathbb{R}^n$ ($n = 2, 3$) is the open bounded domain. The dominant second-order term $\text{div}(\mathbf{a}^\varepsilon \nabla \mathbf{m}^\varepsilon)$ represents the exchange field, where \mathbf{a}^ε is the exchange coefficient. K^ε is the material anisotropy coefficient, and \mathbf{u} denotes the easy-axis direction. \mathbf{h}_a represents the external magnetic field, and M^ε is the magnetization magnitude. In the last term, μ^ε is the material coefficient, and the stray field $\mathbf{h}_d[\mathbf{m}]$ denotes a non-local term derived from the static Maxwell equation. When $n = 3$, for the open bounded domain Ω with Lipschitz boundary, the stray field can be generated by the potential function U^ε

$$(2.2) \quad \begin{cases} \mathbf{h}_d[M^\varepsilon \mathbf{m}^\varepsilon] = \nabla U^\varepsilon, \\ \Delta U^\varepsilon = -\text{div}(M^\varepsilon \mathbf{m}^\varepsilon \cdot \mathcal{X}_\Omega), \end{cases} \quad \text{Stray Field in 3D.}$$

Here, $M^\varepsilon \mathbf{m}^\varepsilon \cdot \mathcal{X}_\Omega$ represents the extension of $M^\varepsilon \mathbf{m}$ to \mathbb{R}^3 , which becomes zero outside Ω . $D'(\mathbb{R}^3)$ denotes a distribution space, which consists of all continuous linear functional of space $C_0^\infty(\mathbb{R}^3)$. When considering the stray field on the thin film ($n=2$), the magnetization component along \mathbf{e}_3 direction disappears. In this case, it has been proved that the stray field degenerates into the simple form [15]

$$(2.3) \quad \mathbf{h}_d[M^\varepsilon \mathbf{m}^\varepsilon] = M^\varepsilon(\mathbf{m}^\varepsilon \cdot \mathbf{e}_3)\mathbf{e}_3, \quad \text{Stray Field in 2D.}$$

Throughout this article, we focus on composite ferromagnetic materials exhibiting the ε -periodic structure. In other words, material coefficients satisfy the following periodic perturbation assumption

$$(2.4) \quad M^\varepsilon = M_s\left(\frac{\mathbf{x}}{\varepsilon}\right), \quad \mu^\varepsilon = \mu\left(\frac{\mathbf{x}}{\varepsilon}\right), \quad \text{and} \quad \mathbf{a}^\varepsilon = \mathbf{a}\left(\frac{\mathbf{x}}{\varepsilon}\right).$$

Here, $M_s(\mathbf{y})$, $\mu(\mathbf{y})$ and $\mathbf{a}(\mathbf{y})$ are periodic functions over the square domain $Y = [0, 1]^n$.

2.1. Two-scale method. In order to address the computational burden of multiscale modeling, the two-scale method is employed to obtain the macroscale and microscale problems corresponding to (1.1). Moreover, the variable separation method

is applied to find the second-order corrector, which satisfies specific geometric constraint. This suitable second-order corrector enables us to conduct the rigorous error analysis in section 3.

2.1.1. Homogenized equation in 3D case. For the 3D case, we rewrite (1.1), (2.1)-(2.3) into a parabolic-elliptic type system

$$(2.5) \quad \begin{cases} \partial_t \mathbf{m}^\varepsilon = \alpha \mathbf{m}^\varepsilon \times \partial_t \mathbf{m}^\varepsilon \\ \quad - (1 + \alpha^2) \mathbf{m}^\varepsilon \times [\operatorname{div}(\mathbf{a}^\varepsilon \nabla \mathbf{m}^\varepsilon) - K^\varepsilon (\mathbf{m}^\varepsilon \cdot \mathbf{u}) \mathbf{u} + M^\varepsilon \mathbf{h}_a + \mu^\varepsilon \nabla U^\varepsilon], \\ \Delta U^\varepsilon = -\operatorname{div}(M^\varepsilon \mathbf{m}^\varepsilon \cdot \mathcal{X}_\Omega), \quad \text{in } D'(\mathbb{R}^3). \end{cases}$$

To utilize the two-scale method, the approximating solution $\tilde{\mathbf{m}}^\varepsilon(\mathbf{x})$ of \mathbf{m}^ε can be defined as

$$(2.6) \quad \begin{cases} \tilde{\mathbf{m}}^\varepsilon(\mathbf{x}) = \mathbf{m}_0\left(\mathbf{x}, \frac{\mathbf{x}}{\varepsilon}\right) + \varepsilon \mathbf{m}_1\left(\mathbf{x}, \frac{\mathbf{x}}{\varepsilon}\right) + \varepsilon^2 \mathbf{m}_2\left(\mathbf{x}, \frac{\mathbf{x}}{\varepsilon}\right), \\ \tilde{U}^\varepsilon(\mathbf{x}) = U_0\left(\mathbf{x}, \frac{\mathbf{x}}{\varepsilon}\right) + \varepsilon U_1\left(\mathbf{x}, \frac{\mathbf{x}}{\varepsilon}\right). \end{cases}$$

Here, $\mathbf{m}_i(\mathbf{x}, \mathbf{y})$ ($i = 0, 1, 2$) is defined over $\Omega \times Y$, and $U_i(\mathbf{x}, \mathbf{y})$ ($i = 0, 1$) is defined over $\mathbb{R}^3 \times Y$. We assume that $\mathbf{m}_i(\mathbf{x}, \mathbf{y})$ and $U_i(\mathbf{x}, \mathbf{y})$ are Y -periodic with respect to \mathbf{y} . Furthermore, \mathbf{m}_i satisfies the geometric ansatz

$$(2.7) \quad |\mathbf{m}_0| = 1, \quad \mathbf{m}_0 \cdot \mathbf{m}_1 = 0, \quad \text{and} \quad \mathbf{m}_0 \cdot \mathbf{m}_2 = -\frac{1}{2} |\mathbf{m}_1|^2.$$

This ansatz constrains the approximating solution $\tilde{\mathbf{m}}^\varepsilon(\mathbf{x})$ such that $|\tilde{\mathbf{m}}^\varepsilon(\mathbf{x})| \approx 1$. Let us denote the fast variable $\mathbf{y} = \frac{\mathbf{x}}{\varepsilon}$ and recall the chain rule

$$(2.8) \quad \nabla \mathbf{m}\left(\mathbf{x}, \frac{\mathbf{x}}{\varepsilon}\right) = (\nabla_{\mathbf{x}} + \varepsilon^{-1} \nabla_{\mathbf{y}}) \mathbf{m}(\mathbf{x}, \mathbf{y}).$$

Then, let $\mathcal{A}_\varepsilon = \operatorname{div}(a^\varepsilon \nabla)$, we have

$$(2.9) \quad \mathcal{A}_\varepsilon \mathbf{m}\left(\mathbf{x}, \frac{\mathbf{x}}{\varepsilon}\right) = (\varepsilon^{-2} \mathcal{A}_0 + \varepsilon^{-1} \mathcal{A}_1 + \mathcal{A}_2) \mathbf{m}(\mathbf{x}, \mathbf{y}),$$

where

$$(2.10) \quad \begin{cases} \mathcal{A}_0 = \operatorname{div}_{\mathbf{y}}(\mathbf{a}(\mathbf{y}) \nabla_{\mathbf{y}}), \\ \mathcal{A}_1 = \operatorname{div}_{\mathbf{x}}(\mathbf{a}(\mathbf{y}) \nabla_{\mathbf{y}}) + \operatorname{div}_{\mathbf{y}}(\mathbf{a}(\mathbf{y}) \nabla_{\mathbf{x}}), \\ \mathcal{A}_2 = \operatorname{div}_{\mathbf{x}}(\mathbf{a}(\mathbf{y}) \nabla_{\mathbf{x}}). \end{cases}$$

Substituting (2.9) into (2.5), the ε^{-2} -order equation can be written as

$$\mathbf{m}_0 \times \mathcal{A}_0 \mathbf{m}_0 = 0, \quad \Delta_{\mathbf{y}} U_0 = 0.$$

The equation can be easily checked by setting $\mathbf{m}_0(\mathbf{x}, \mathbf{y}) = \mathbf{m}_0(\mathbf{x})$ and $U_0(\mathbf{x}, \mathbf{y}) = U_0(\mathbf{x})$. In fact, one can prove the uniqueness of the solution (up to a constant) by the Lax-Milgram Theorem and the same argument as in [9]. Using the above results, the ε^{-1} -order equation can be given as

$$\begin{cases} \mathbf{m}_0 \times (\mathcal{A}_1 \mathbf{m}_0 + \mathcal{A}_0 \mathbf{m}_1) = 0, \\ \Delta_{\mathbf{y}} U_1(\mathbf{x}, \mathbf{y}) + \nabla_{\mathbf{y}} M_s(\mathbf{y}) \cdot (\mathbf{m}_0(\mathbf{x}) \mathcal{X}_\Omega(\mathbf{x})) = 0. \end{cases}$$

Here, the first-order correctors \mathbf{m}_1 and U_1 are defined as

$$(2.11) \quad \mathbf{m}_1(\mathbf{x}, \mathbf{y}) = \sum_{j=1}^3 \chi_j(\mathbf{y}) \frac{\partial}{\partial x_j} \mathbf{m}_0(\mathbf{x}), \quad U_1(\mathbf{x}, \mathbf{y}) = \mathbf{u}(\mathbf{y}) \cdot \mathbf{m}_0(\mathbf{x}) \mathcal{X}_\Omega(\mathbf{x}),$$

where $\chi_i(\mathbf{y})$, $i = 1, 2, 3$, and $\mathbf{u}(\mathbf{y}) = \nabla U^*(\mathbf{y})$ are the auxiliary functions satisfying the first-order cell problem

$$(2.12) \quad \begin{cases} \operatorname{div}(\mathbf{a}(\mathbf{y}) \nabla \chi_j(\mathbf{y})) = - \sum_{i=1}^3 \frac{\partial}{\partial y_i} a_{ij}(\mathbf{y}), & \chi_j \text{ is } Y\text{-periodic,} \\ \Delta U^*(\mathbf{y}) = -M_s(\mathbf{y}) + M^0, & U^* \text{ is } Y\text{-periodic, } M^0 = \int_Y M_s(\mathbf{y}) \, d\mathbf{y}. \end{cases}$$

Furthermore, the property $\mathbf{m}_0 \cdot \mathbf{m}_1 = 0$ holds under the assumption $|\mathbf{m}_0| = 1$. Now, let us denote

$$(2.13) \quad \mathbf{h}(\mathbf{x}, \mathbf{y}) = \mathcal{A}_1 \mathbf{m}_1 + \mathcal{A}_2 \mathbf{m}_0 + \mu \nabla_{\mathbf{x}} U_0 + \mu \nabla_{\mathbf{y}} U_1 - K(\mathbf{m}_0 \cdot \mathbf{u}) \mathbf{u} + M_s \mathbf{h}_a,$$

the ε^0 -order equation can be given as

$$(2.14) \quad \begin{cases} \partial_t \mathbf{m}_0 - \alpha \mathbf{m}_0 \times \partial_t \mathbf{m}_0 = -(1 + \alpha^2) \mathbf{m}_0 \times \{\mathcal{A}_0 \mathbf{m}_2 + \mathbf{h}(\mathbf{x}, \mathbf{y})\}, \\ \Delta_{\mathbf{x}} U_0 + 2 \operatorname{div}_{\mathbf{y}}(\nabla_{\mathbf{x}} U_1) + M_s \operatorname{div}_{\mathbf{x}}(\mathbf{m}_0 \mathcal{X}_\Omega(\mathbf{x})) + \operatorname{div}_{\mathbf{y}}(M_s \mathbf{m}_1 \mathcal{X}_\Omega(\mathbf{x})) = 0. \end{cases}$$

Taking integration of (2.14) with respect to \mathbf{y} over Y , the corresponding homogenized LLG equation can be obtained as

$$(2.15) \quad \begin{cases} \partial_t \mathbf{m}_0 - \alpha \mathbf{m}_0 \times \partial_t \mathbf{m}_0 = -(1 + \alpha^2) \mathbf{m}_0 \times \mathbf{h}_{\text{eff}}^0, \\ \Delta U_0(\mathbf{x}) = -M^0 \operatorname{div}_{\mathbf{x}}(\mathbf{m}_0 \mathcal{X}_\Omega(\mathbf{x})), \end{cases}$$

with $\mathbf{h}_{\text{eff}}^0(\mathbf{x}) = \int_Y \mathbf{h}(\mathbf{x}, \mathbf{y}) \, d\mathbf{y}$, which can be computed by

$$(2.16) \quad \mathbf{h}_{\text{eff}}^0 = \operatorname{div}(\mathbf{a}^0 \nabla \mathbf{m}_0) + \mu^0 \nabla U^0 + \mathbf{m}_0 \cdot \mathbf{H}_d^0 - K^0(\mathbf{m}_0 \cdot \mathbf{u}) \mathbf{u} + M^0 \mathbf{h}_a.$$

Here, the homogenized coefficients $\mathbf{a}^0 = \{a_{ij}^0\}_{1 \leq i, j \leq 3}$, μ^0 , K^0 and matrix \mathbf{H}_d^0 are given by

$$(2.17) \quad \begin{cases} a_{ij}^0 = \int_Y \left(a_{ij} + \sum_{k=1}^3 a_{ik} \frac{\partial \chi_j}{\partial y_k} \right) d\mathbf{y}, & \mu^0 = \int_Y \mu(\mathbf{y}) \, d\mathbf{y}, \\ K^0 = \int_Y K(\mathbf{y}) \, d\mathbf{y}, & \mathbf{H}_d^0 = \int_Y \mu(\mathbf{y}) \nabla \mathbf{u}(\mathbf{y}) \, d\mathbf{y}. \end{cases}$$

The second-order corrector $\mathbf{m}_2(\mathbf{x}, \mathbf{y})$ are given as follows. Combining (2.14) with the homogenized equation (2.15), it yields

$$(2.18) \quad \mathbf{m}_0 \times \{\mathcal{A}_0 \mathbf{m}_2 + \mathbf{h}(\mathbf{x}, \mathbf{y}) - \mathbf{h}_{\text{eff}}^0(\mathbf{x})\} = 0.$$

Under the ansatz $\mathbf{m}_2 \cdot \mathbf{m}_0 = -\frac{1}{2} |\mathbf{m}_1|^2$ in (2.7), we have

$$(2.19) \quad \mathbf{m}_0 \cdot \mathcal{A}_0 \mathbf{m}_2 = -\mathbf{a}(\mathbf{y}) \nabla_{\mathbf{y}} \mathbf{m}_1 \cdot \nabla_{\mathbf{y}} \mathbf{m}_1 - \mathbf{m}_1 \cdot \mathcal{A}_0 \mathbf{m}_1.$$

Using the orthogonal decomposition of $\mathcal{A}_0 \mathbf{m}_2$, together with (2.18) and (2.19), it yields

$$(2.20) \quad \begin{aligned} \mathcal{A}_0 \mathbf{m}_2 &= -\mathbf{m}_0 \times (\mathbf{m}_0 \times \mathcal{A}_0 \mathbf{m}_2) + (\mathbf{m}_0 \cdot \mathcal{A}_0 \mathbf{m}_2) \mathbf{m}_0 \\ &= -(\mathbf{h}(\mathbf{x}, \mathbf{y}) - \mathbf{h}_{\text{eff}}^0(\mathbf{x})) + \{\mathbf{m}_0 \cdot (\mathbf{h}(\mathbf{x}, \mathbf{y}) - \mathbf{h}_{\text{eff}}^0(\mathbf{x}))\} \mathbf{m}_0 \\ &\quad - (\mathbf{m}_1 \cdot \mathcal{A}_0 \mathbf{m}_1 + \mathbf{a}(\mathbf{y}) \nabla_{\mathbf{y}} \mathbf{m}_1 \cdot \nabla_{\mathbf{y}} \mathbf{m}_1) \mathbf{m}_0. \end{aligned}$$

By the variable separation method, the solution of (2.20) is given by (2.21)

$$(2.21) \quad \begin{aligned} \mathbf{m}_2(\mathbf{x}, \mathbf{y}) &= \text{div}_{\mathbf{x}}(\boldsymbol{\theta}(\mathbf{y}) \nabla_{\mathbf{x}} \mathbf{m}_0(\mathbf{x})) + \left\{ (\boldsymbol{\theta}(\mathbf{y}) + \frac{1}{2} \boldsymbol{\chi}(\mathbf{y}) \otimes \boldsymbol{\chi}(\mathbf{y})) |\nabla \mathbf{m}_0(\mathbf{x})|^2 \right\} \mathbf{m}_0(\mathbf{x}) \\ &\quad + (I - \mathbf{m}_0(\mathbf{x}) \otimes \mathbf{m}_0(\mathbf{x})) \mathcal{T}_{\text{low}}(\mathbf{x}, \mathbf{y}), \end{aligned}$$

where I is the identity transformation, \otimes denotes the tensor product, and the low-order term \mathcal{T}_{low} is given by

$$\mathcal{T}_{\text{low}}(\mathbf{x}, \mathbf{y}) = -\kappa(\mathbf{y})(\mathbf{m}_0(\mathbf{x}) \cdot \mathbf{u}) \mathbf{u} + \rho(\mathbf{y}) \nabla_{\mathbf{x}} U_0(\mathbf{x}) + \mathbf{m}_0(\mathbf{x}) \cdot \boldsymbol{\Lambda}(\mathbf{y}) + U^*(\mathbf{y}) \mathbf{h}_a.$$

Here, $U^*(\mathbf{y})$ is defined in (2.12). The auxiliary functions $\boldsymbol{\theta} = \{\theta_{ij}\}_{1 \leq i, j \leq 3}$, ρ , $\boldsymbol{\Lambda}$, κ are given by the second-order cell problem

$$(2.22) \quad \begin{cases} \mathcal{A}_0 \theta_{ij} = a_{ij}^0 - \left(a_{ij} + \sum_{k=1}^3 a_{ik} \frac{\partial \chi_j}{\partial y_k} \right) - \sum_{k=1}^3 \frac{\partial (a_{ik} \chi_j)}{\partial y_k}, \\ \mathcal{A}_0 \rho = \mu(\mathbf{y}) - \mu^0, \quad \mathcal{A}_0 \boldsymbol{\Lambda} = \mu(\mathbf{y}) \nabla \mathbf{u}(\mathbf{y}) - \mathbf{H}_d^0, \\ \mathcal{A}_0 \kappa = K(\mathbf{y}) - K^0, \\ \boldsymbol{\theta}, \rho, \boldsymbol{\Lambda}, \kappa, \quad \text{are } Y\text{-periodic.} \end{cases}$$

2.1.2. Homogenized equation in 2D case. For the 2D case, we can apply the same argument for the multiscale equation (1.1), (2.1) with the degenerated stray field (2.3). The homogenized equation reads as

$$\partial_t \mathbf{m}_0 - \alpha \mathbf{m}_0 \times \partial_t \mathbf{m}_0 = -(1 + \alpha^2) \mathbf{m}_0 \times \mathbf{h}_{\text{eff}}^0,$$

where the homogenized effective field $\mathbf{h}_{\text{eff}}^0$ is given by

$$(2.23) \quad \mathbf{h}_{\text{eff}}^0 = \text{div}(\mathbf{a}^0 \nabla \mathbf{m}_0) + \widetilde{M}^0 (\mathbf{m}^\varepsilon \cdot \mathbf{e}_3) \mathbf{e}_3 - K^0 (\mathbf{m}_0 \cdot \mathbf{u}) \mathbf{u} + M^0 \mathbf{h}_a,$$

with $\mathbf{a}^0 = \{a_{ij}^0\}_{1 \leq i, j \leq 3}$, μ^0 , K^0 defined in (2.17), and \widetilde{M}^0 is given by

$$\widetilde{M}^0 = \int_Y \mu(\mathbf{y}) M_s(\mathbf{y}) d\mathbf{y}.$$

Moreover, the second order corrector can also be written in the form of (2.21), with the low-order term $\mathcal{T}_{\text{low}}(\mathbf{x}, \mathbf{y})$ given by

$$\begin{aligned} \mathcal{T}_{\text{low}}(\mathbf{x}, \mathbf{y}) &= -\kappa(\mathbf{y})(\mathbf{m}_0(\mathbf{x}) \cdot \mathbf{u}) \mathbf{u} + \beta(\mathbf{y})(\mathbf{m}_0(\mathbf{x}) \cdot \mathbf{e}_3) \mathbf{e}_3 + \rho(\mathbf{y}) \nabla_{\mathbf{x}} U_0(\mathbf{x}) \\ &\quad + \mathbf{m}_0(\mathbf{x}) \cdot \boldsymbol{\Lambda}(\mathbf{y}) + U^*(\mathbf{y}) \mathbf{h}_a. \end{aligned}$$

Here, $\beta(\mathbf{y})$ is a Y -periodic function satisfying the second-order cell problem

$$\mathcal{A}_0 \beta(\mathbf{y}) = \mu(\mathbf{y}) M_s(\mathbf{y}) - \widetilde{M}^0.$$

2.2. Boundary value problems. In this work, we consider two types of the boundary value problem: the Periodic problem and the Neumann problem. First, for $\Omega = [0, 1]^n$, the multiscale problem (1.1) with periodic boundary setting is defined as

$$(2.24) \quad \begin{cases} \partial_t \mathbf{m}^\varepsilon - \alpha \mathbf{m}^\varepsilon \times \partial_t \mathbf{m}^\varepsilon = - (1 + \alpha^2) \mathbf{m}^\varepsilon \times \mathbf{h}_{\text{eff}}^\varepsilon(\mathbf{m}^\varepsilon) & \text{in } \Omega, \\ \mathbf{m}^\varepsilon(\mathbf{x}, 0) = \mathbf{m}_{\text{init}}^\varepsilon(\mathbf{x}), \quad |\mathbf{m}_{\text{init}}^\varepsilon(\mathbf{x})| = 1 & \text{in } \Omega, \\ \mathbf{m}^\varepsilon(\mathbf{x}, t), \quad \mathbf{m}_{\text{init}}^\varepsilon(\mathbf{x}) & \text{are periodic on } \partial\Omega, \end{cases}$$

where $\mathbf{m}_{\text{init}}^\varepsilon(\mathbf{x})$ is initial condition, and the effective field $\mathbf{h}_{\text{eff}}^\varepsilon(\mathbf{m}^\varepsilon)$ is given in (2.1)-(2.3). The corresponding homogenized problem with periodic boundary can be written as

$$(2.25) \quad \begin{cases} \partial_t \mathbf{m}_0 - \alpha \mathbf{m}_0 \times \partial_t \mathbf{m}_0 = - (1 + \alpha^2) \mathbf{m}_0 \times \mathbf{h}_{\text{eff}}^0(\mathbf{m}_0) & \text{in } \Omega, \\ \mathbf{m}_0(\mathbf{x}, 0) = \mathbf{m}_{\text{init}}^0(\mathbf{x}), \quad |\mathbf{m}_{\text{init}}^0(\mathbf{x})| = 1 & \text{in } \Omega, \\ \mathbf{m}_0(\mathbf{x}, t), \quad \mathbf{m}_{\text{init}}^0(\mathbf{x}) & \text{are periodic on } \partial\Omega, \end{cases}$$

where $\mathbf{m}_{\text{init}}^0(\mathbf{x})$ is the initial condition, and the homogenized effective field $\mathbf{h}_{\text{eff}}^0(\mathbf{m}_0)$ is defined in (2.16), (2.23). The multiscale solution \mathbf{m}^ε can be approximated by \mathbf{m}_0 of (2.25) and the first-order corrector \mathbf{m}^1 of (2.11) in the following form

$$(2.26) \quad \mathbf{m}^\varepsilon(\mathbf{x}) \approx \mathbf{m}_0(\mathbf{x}) + \varepsilon \chi\left(\frac{\mathbf{x}}{\varepsilon}\right) \nabla \mathbf{m}_0(\mathbf{x}).$$

The two-scale convergence of approximation (2.26) has been proved in [26, 1, 11, 9]. Suppose only the exchange field is considered in (2.24), and \mathbf{m}^ε satisfies the certain boundedness assumption. In this case, it has been proved that (2.26) has the convergence order $O(\varepsilon)$ in the $L^2(\Omega)$ sense and remains uniformly bounded in the $H^1(\Omega)$ sense [20].

On the other hand, for an open bounded domain Ω , the multiscale problem (1.1) with Neumann boundary setting is defined as

$$(2.27) \quad \begin{cases} \partial_t \mathbf{m}^\varepsilon - \alpha \mathbf{m}^\varepsilon \times \partial_t \mathbf{m}^\varepsilon = - (1 + \alpha^2) \mathbf{m}^\varepsilon \times \mathbf{h}_{\text{eff}}^\varepsilon(\mathbf{m}^\varepsilon) & \text{in } \Omega, \\ \mathbf{m}^\varepsilon(\mathbf{x}, 0) = \mathbf{m}_{\text{init}}^\varepsilon(\mathbf{x}), \quad |\mathbf{m}_{\text{init}}^\varepsilon(\mathbf{x})| = 1 & \text{in } \Omega, \\ \boldsymbol{\nu} \cdot \mathbf{a}^\varepsilon \nabla \mathbf{m}^\varepsilon(\mathbf{x}, t) = 0, & \text{on } \partial\Omega \times [0, T], \\ \boldsymbol{\nu} \cdot \mathbf{a}^\varepsilon \nabla \mathbf{m}_{\text{init}}^\varepsilon(\mathbf{x}) = 0, & \text{on } \partial\Omega, \end{cases}$$

where $\boldsymbol{\nu}$ represents the unit outer normal vector. The corresponding homogenized Neumann problem is given by

$$(2.28) \quad \begin{cases} \partial_t \mathbf{m}_0 - \alpha \mathbf{m}_0 \times \partial_t \mathbf{m}_0 = - (1 + \alpha^2) \mathbf{m}_0 \times \mathbf{h}_{\text{eff}}^0(\mathbf{m}_0) & \text{in } \Omega, \\ \mathbf{m}_0(\mathbf{x}, 0) = \mathbf{m}_{\text{init}}^0(\mathbf{x}), \quad |\mathbf{m}_{\text{init}}^0(\mathbf{x})| = 1 & \text{in } \Omega, \\ \boldsymbol{\nu} \cdot \mathbf{a}^0 \nabla \mathbf{m}_0(\mathbf{x}, t) = 0, & \text{on } \partial\Omega \times [0, T], \\ \boldsymbol{\nu} \cdot \mathbf{a}^0 \nabla \mathbf{m}_{\text{init}}^0(\mathbf{x}) = 0, & \text{on } \partial\Omega. \end{cases}$$

For the Neumann problem, the convergence order in the H^1 sense of (2.26) has been derived without considering the boundary layer effect [10]. Moreover, to approximate the multiscale solution more accurately, the Neumann corrector $\boldsymbol{\Phi}^\varepsilon = \{\Phi_i^\varepsilon\}_{i=1}^n$ was introduced

$$(2.29) \quad \begin{cases} \operatorname{div}(\mathbf{a}^\varepsilon \nabla \Phi_i^\varepsilon) = \operatorname{div}(\mathbf{a}^0 \nabla x_i) = 0 & \text{in } \Omega, \\ \boldsymbol{\nu} \cdot \mathbf{a}^\varepsilon \nabla \Phi_i^\varepsilon = \boldsymbol{\nu} \cdot \mathbf{a}^0 \nabla x_i & \text{on } \partial\Omega. \end{cases}$$

Here, x_i is the i -th component of the spatial variable \mathbf{x} , which can be seen as the homogenized solution of Φ_i^ε . To make Φ_i^ε be unique up to a constant, it is assumed that $\Phi_i^\varepsilon(\tilde{\mathbf{x}}) - \tilde{\mathbf{x}} = 0$ for some $\tilde{\mathbf{x}} \in \Omega$. Utilizing the Neumann corrector Φ^ε , [10] provided a sharper estimation for the approximation

$$(2.30) \quad \mathbf{m}^\varepsilon \approx \mathbf{m}_0 + (\Phi^\varepsilon - \mathbf{x}) \nabla \mathbf{m}_0.$$

In this work, the full system in (2.24) is considered, and the convergence order of approximation (2.26) in the $H^1(\Omega)$ sense is derived.

2.3. Initial data. To examine the asymptotic behavior of the solution from the multiscale system to the homogenized system under (2.26) and (2.30), it is natural to propose the same initial data, i.e. $\mathbf{m}_{\text{init}}^\varepsilon = \mathbf{m}_{\text{init}}^0$. However, this simple setting may violate the consistency of the boundary condition, because of $\boldsymbol{\nu} \cdot \mathbf{a}^\varepsilon \nabla \mathbf{m}_{\text{init}}^\varepsilon \neq \boldsymbol{\nu} \cdot \mathbf{a}^0 \nabla \mathbf{m}_{\text{init}}^0$ for the Neumann problem. To address this problem, we can apply the following strategy to determine the proper initial data. Given a smooth function $\mathbf{m}_{\text{init}}^0 \in S^2$ of the homogenized problem such that the consistency condition holds, then $\mathbf{m}_{\text{init}}^\varepsilon \in S^2$ is defined by the non-homogeneous multiscale harmonic mapping

$$(2.31) \quad \begin{cases} \mathbf{m}_{\text{init}}^\varepsilon \times (\mathcal{A}_\varepsilon \mathbf{m}_{\text{init}}^\varepsilon - \mathcal{A}^0 \mathbf{m}_{\text{init}}^0) = 0, \\ |\mathbf{m}_{\text{init}}^\varepsilon| = 1, \\ \boldsymbol{\nu} \cdot \mathbf{a}^\varepsilon \nabla \mathbf{m}_{\text{init}}^\varepsilon = 0, \quad \text{or} \quad \mathbf{m}_{\text{init}}^\varepsilon \text{ is periodic on } \partial\Omega. \end{cases}$$

By taking the outer product of both sides of (2.31) with $\mathbf{m}_{\text{init}}^\varepsilon(\mathbf{x})$, (2.31) can be rewritten as

$$(2.32) \quad \mathcal{A}_\varepsilon \mathbf{m}_{\text{init}}^\varepsilon = \mathbf{m}_{\text{init}}^\varepsilon \times (\mathbf{m}_{\text{init}}^\varepsilon \times \mathcal{A}^0 \mathbf{m}_{\text{init}}^0) - \mathbf{a}^\varepsilon |\nabla \mathbf{m}_{\text{init}}^\varepsilon|^2 \mathbf{m}_{\text{init}}^\varepsilon.$$

Then, (2.32) can be simplified with the vector triple product formula

$$(2.33) \quad \boldsymbol{\eta} \times (\boldsymbol{\nu} \times \boldsymbol{\zeta}) = (\boldsymbol{\eta} \cdot \boldsymbol{\zeta}) \boldsymbol{\nu} - (\boldsymbol{\eta} \cdot \boldsymbol{\nu}) \boldsymbol{\zeta}, \quad \forall \boldsymbol{\eta}, \boldsymbol{\nu}, \boldsymbol{\zeta}.$$

Finally, the variational form of (2.32) can be expressed as

$$(2.34) \quad \begin{aligned} (\mathbf{a}^\varepsilon \nabla \mathbf{m}_{\text{init}}^\varepsilon, \nabla \mathbf{v}) &= -(\mathbf{F}, \mathbf{v}) + ((\mathbf{m}_{\text{init}}^\varepsilon \cdot \mathbf{F}) \mathbf{m}_{\text{init}}^\varepsilon, \mathbf{v}) \\ &\quad - \left(\left\{ \sum a_{ij}^\varepsilon (\partial_i \mathbf{m}_{\text{init}}^\varepsilon \cdot \partial_j \mathbf{m}_{\text{init}}^\varepsilon) \right\} \mathbf{m}_{\text{init}}^\varepsilon, \mathbf{v} \right), \quad \forall \mathbf{v} \in H^1(\Omega), \end{aligned}$$

where $\mathbf{F} = \text{div}(\mathbf{a}^0 \nabla \mathbf{m}_{\text{init}}^0)$. The equation (2.34) is named as the projection method, such that the computed magnetic moment is located on the unit sphere. However, due to the nonlinearity, (2.34) cannot be directly solved in closed form. Therefore, iteration methods, such as the Picard iteration, can be applied to obtain the desired solution. These methods not only require multiple iterations but also require suitable initial guesses to ensure convergence, significantly increasing the computational complexity.

To overcome the above difficulties, we design the expansion method, where the two-scale method is utilized on the initial data. Given a smooth function $\mathbf{m}_{\text{init}}^0(\mathbf{x}) \in S^2$ of the homogenized problem, $\mathbf{m}_{\text{init}}^\varepsilon$ is defined as

$$(2.35) \quad \mathbf{m}_{\text{init}}^\varepsilon(\mathbf{x}) = \mathbf{m}_{\text{init}}^0(\mathbf{x}) + \tilde{\mathbf{m}}_{\text{init}}^\varepsilon \left(\mathbf{x}, \frac{\mathbf{x}}{\varepsilon} \right),$$

where $\tilde{\mathbf{m}}_{\text{init}}^c(\mathbf{x}, \mathbf{y})$ is the correction term related to the boundary conditions of the multiscale equation, which can be represented as

$$(2.36) \quad \tilde{\mathbf{m}}_{\text{init}}^c(\mathbf{x}, \mathbf{y}) = \begin{cases} \varepsilon \chi \left(\frac{\mathbf{x}}{\varepsilon} \right) \nabla \mathbf{m}_{\text{init}}^0(\mathbf{x}), & \text{with Periodic boundary,} \\ (\Phi^\varepsilon - \mathbf{x}) \nabla \mathbf{m}_{\text{init}}^0(\mathbf{x}), & \text{with Neumann boundary.} \end{cases}$$

It can be proved that the initial data $\mathbf{m}_{\text{init}}^\varepsilon$ in (2.35) satisfies the consistency of the boundary condition. Specifically, for the Neumann problem, we have $\boldsymbol{\nu} \cdot \mathbf{a}^\varepsilon \nabla \mathbf{m}_{\text{init}}^\varepsilon = \boldsymbol{\nu} \cdot \mathbf{a}^0 \nabla \mathbf{m}_{\text{init}}^0$. However, $\mathbf{m}_{\text{init}}^\varepsilon$ is not sphere-valued, which satisfies

$$|\mathbf{m}_{\text{init}}^\varepsilon|^2 = |\mathbf{m}_{\text{init}}^0|^2 + |\tilde{\mathbf{m}}_{\text{init}}^c|^2 = 1 + |\tilde{\mathbf{m}}_{\text{init}}^c|^2.$$

Then, we have

$$|\mathbf{m}_{\text{init}}^\varepsilon| - 1 = \frac{|\tilde{\mathbf{m}}_{\text{init}}^c|^2}{|\mathbf{m}_{\text{init}}^\varepsilon| + 1},$$

where $|\mathbf{m}_{\text{init}}^\varepsilon| - 1$ is non-zero but $O(|\tilde{\mathbf{m}}_{\text{init}}^c|^2)$. Compared with the projection method (2.34), the expansion method provides the initial data of the multiscale system in explicit form, significantly improving the computational efficiency. In this work, we apply the initial setting (2.31) for the theoretical analysis, and apply setting (2.35) for the numerical simulations.

2.4. Numerical scheme. In this subsection, we design an improved implicit numerical scheme to solve the homogenized LLG equation (2.15). The same scheme can be applied to solve the multiscale LLG equation (1.1), the first-order cell problem (2.12), and the second-order cell problem (2.22).

In the spatial discretization, the finite element method is employed for each component of the homogenized magnetic moment \mathbf{m}_0 . Given the lowest order finite element space $V_h \subset W^{1,2}(\Omega; \mathbb{R}^3)$ subordinate to the triangulation T_h of the domain Ω , the variational form reads as follows: To find $\mathbf{m}_{0,h} \in V_h$, such that

$$(2.37) \quad \begin{aligned} & (\partial_t \mathbf{m}_{0,h}, \mathbf{v}_h)_h - \alpha (\mathbf{m}_{0,h} \times \partial_t \mathbf{m}_{0,h}, \mathbf{v}_h)_h \\ &= - (1 + \alpha^2) (\mathbf{m}_{0,h} \times \mathbf{h}_{\text{eff}}^0(\mathbf{m}_{0,h}), \mathbf{v}_h)_h, \end{aligned} \quad \forall \mathbf{v}_h \in \mathbf{V}_h,$$

where $(\cdot, \cdot)_h$ represents the discrete inner product in $L^2(\Omega)$.

In the temporal discretization, implicit and semi-implicit schemes have often been used due to their unconditional numerical stability [17]. In more details, the implicit schemes preserve the magnetization's magnitude and the Lyapunov structure of the LLG equation. The work [4] provided an effective implicit temporal discretization scheme

$$(2.38) \quad \begin{aligned} & \frac{1}{\Delta t} (\mathbf{m}_{0,h}^{j+1}, \mathbf{v}_h)_h - \frac{\alpha}{\Delta t} (\mathbf{m}_{0,h}^j \times \mathbf{m}_{0,h}^{j+1}, \mathbf{v}_h)_h \\ &= \frac{1}{\Delta t} (\mathbf{m}_{0,h}^j, \mathbf{v}_h)_h - (1 + \alpha^2) (\overline{\mathbf{m}}_{0,h}^{j+1/2} \times \mathbf{h}_{\text{eff}}^0(\overline{\mathbf{m}}_{0,h}^{j+1/2}), \mathbf{v}_h)_h, \end{aligned} \quad \forall \mathbf{v}_h \in \mathbf{V}_h,$$

where Δt is the time step size, $\mathbf{m}_{0,h}^j$ and $\overline{\mathbf{m}}_{0,h}^{j+1/2}$ are defined as

$$\begin{aligned} \mathbf{m}_{0,h}^j &:= \mathbf{m}_{0,h}^j(\mathbf{x}, j\Delta t), \\ \overline{\mathbf{m}}_{0,h}^{j+1/2} &:= (\mathbf{m}_{0,h}^{j+1} + \mathbf{m}_{0,h}^j)/2, \end{aligned} \quad j = 0, 1, 2, \dots$$

To handle the nonlinear system in (2.38), a implicit iteration scheme was employed in each time step

$$\begin{aligned}
(2.39) \quad & \frac{1}{\Delta t} (\mathbf{m}_{0,h}^{j+1,\ell+1}, \mathbf{v}_h)_h - \frac{\alpha}{\Delta t} (\mathbf{m}_{0,h}^j \times \mathbf{m}_{0,h}^{j+1,\ell+1}, \mathbf{v}_h)_h \\
& + \frac{1+\alpha^2}{4} (\mathbf{m}_{0,h}^{j+1,\ell+1} \times \mathbf{h}_{\text{eff}}^0(\mathbf{m}_{0,h}^{j+1,\ell}), \mathbf{v}_h)_h + \frac{1+\alpha^2}{4} (\mathbf{m}_{0,h}^{j+1,\ell+1} \times \mathbf{h}_{\text{eff}}^0(\mathbf{m}_{0,h}^j), \mathbf{v}_h)_h \\
& + \frac{1+\alpha^2}{4} (\mathbf{m}_{0,h}^j \times \mathbf{h}_{\text{eff}}^0(\mathbf{m}_{0,h}^{j+1,\ell+1}), \mathbf{v}_h)_h \\
= & \frac{1}{\Delta t} (\mathbf{m}_{0,h}^j, \mathbf{v}_h)_h - \frac{1+\alpha^2}{4} (\mathbf{m}_{0,h}^j \times \mathbf{h}_{\text{eff}}^0(\mathbf{m}_{0,h}^j), \mathbf{v}_h)_h, \quad \forall \mathbf{v}_h \in \mathbf{V}_h, \quad \ell = 0, 1, 2, \dots
\end{aligned}$$

where ℓ denotes the ℓ -th iteration step. The equation (2.39) has a unique solution when the following condition is satisfied

$$(2.40) \quad \Delta t \leq \frac{h^2}{10(1+\alpha^2)}.$$

where h is the spatial mesh size. However, convergence efficiency has always been the emphasis to optimize the above scheme.

Based on the temporal discretization scheme (2.38), an improved implicit scheme is designed, and a novel semi-implicit iteration scheme is employed to handle the corresponding nonlinear system. The semi-implicit iteration scheme is given by

$$\begin{aligned}
(2.41) \quad & \frac{1}{\Delta t} (\mathbf{m}_{0,h}^{j+1,\ell+1}, \mathbf{v}_h)_h - \frac{\alpha}{\Delta t} (\mathbf{m}_{0,h}^j \times \mathbf{m}_{0,h}^{j+1,\ell+1}, \mathbf{v}_h)_h \\
& + \frac{1+\alpha^2}{4} (\mathbf{m}_{0,h}^{j+1,\ell} \times \mathbf{h}_{\text{eff}}^0(\mathbf{m}_{0,h}^{j+1,\ell+1}), \mathbf{v}_h)_h + \frac{1+\alpha^2}{4} (\mathbf{m}_{0,h}^{j+1,\ell+1} \times \mathbf{h}_{\text{eff}}^0(\mathbf{m}_{0,h}^j), \mathbf{v}_h)_h \\
& + \frac{1+\alpha^2}{4} (\mathbf{m}_{0,h}^j \times \mathbf{h}_{\text{eff}}^0(\mathbf{m}_{0,h}^{j+1,\ell+1}), \mathbf{v}_h)_h \\
= & \frac{1}{\Delta t} (\mathbf{m}_{0,h}^j, \mathbf{v}_h)_h - \frac{1+\alpha^2}{4} (\mathbf{m}_{0,h}^j \times \mathbf{h}_{\text{eff}}^0(\mathbf{m}_{0,h}^j), \mathbf{v}_h)_h, \quad \forall \mathbf{v}_h \in \mathbf{V}_h, \quad \ell = 0, 1, 2, \dots
\end{aligned}$$

For the original scheme (2.38),(2.39) and the improved scheme (2.38),(2.41), the converge time and iteration steps of the corresponding nonlinear system are depicted in Table 1. The table shows that the improved scheme significantly reduces the number of iteration steps and relaxes the constraints on the time step size, enabling it to handle the multiscale LLG equation.

Δt	original scheme [4]		improved scheme	
	time(s)	iteration steps	time(s)	iteration steps
10^{-4}	-	-	49.2	9
10^{-5}	352.2	58	33.4	6
10^{-6}	54.8	10	22.8	4

Table 1: Comparison of the converge time and iteration steps for two numerical schemes. The spatial mesh size is $h = \frac{1}{180}$, - represents that the scheme does not converge under the time step size Δt .

2.5. The flowchart of the algorithm. By combining the aforementioned two-scale method with the corresponding numerical scheme, the algorithm for solving (1.1) is summarized in Algorithm 2.1.

Algorithm 2.1 The flowchart of the algorithm to solve (1.1) with two-scale method.

Input: $\mathbf{m}_{0,h}^0 = \mathbf{m}_{\text{init}}^0(\mathbf{x})$, $T = N_t k$, all parameters need;

Output: $\{\tilde{\mathbf{m}}_h^{\varepsilon,j}\}_{j=0,1,\dots,N_t}$;

- 1: Get the initial value $\tilde{\mathbf{m}}_{\text{init}}^{\varepsilon}(\mathbf{x})$ of the multiscale LLG equation by (2.35);
 - 2: Solve the first-order cell problem (2.12) to get the auxiliary functions χ and U^* ;
 - 3: Compute the homogenized coefficient \mathbf{a}^0, μ^0, K^0 and \mathbf{H}_d^0 based on (2.17);
 - 4: Solve the second-order cell problem (2.22) to get the auxiliary functions θ, ρ, Λ and κ ;
 - 5: Let $j = 0$;
 - 6: **while** $j < N_t$ **do**
 - 7: Let $\ell = 0$, $\mathbf{m}_{0,h}^{j+1,0} = \mathbf{m}_{0,h}^j$;
 - 8: Calculate $\mathbf{m}_{0,h}^{j+1,1}$ by solving (2.41);
 - 9: **while** $\|\mathbf{m}_{0,h}^{j+1,\ell+1} - \mathbf{m}_{0,h}^{j+1,\ell}\| \geq \text{threshold}$ **do**
 - 10: Let $\ell = \ell + 1$;
 - 11: Calculate $\mathbf{m}_{0,h}^{j+1,\ell+1}$ by solving (2.41);
 - 12: **end while**
 - 13: Update $\mathbf{m}_{0,h}^{j+1} = \mathbf{m}_{0,h}^{j+1,\ell}$;
 - 14: Let $j = j + 1$;
 - 15: **end while**
 - 16: Utilize (2.11) to get the first-order correctors \mathbf{m}_1 and U_1 ;
 - 17: Use (2.21) to get the second-order corrector \mathbf{m}_2 ;
 - 18: Assemble the approximate solution $\{\tilde{\mathbf{m}}_h^{\varepsilon,j}\}_{j=0,1,\dots,N_t}$ based on (2.6).
-

Remark 2.1. As the auxiliary functions are independent of the time variable, the cell problems (2.12) and (2.22) only need to be computed once throughout the process.

3. Convergence analysis under different effective fields and boundary corrections. In this section, we present some theoretical results for both the Periodic and Neumann problems. For the Periodic problem, the new convergence results are presented in Theorem 3.1 of subsection 3.1, and the corresponding detailed proof is given in subsection 3.2. For the Neumann problem, the results are presented in Proposition 3.2 and Proposition 3.3 of subsection 3.1. Theoretical results for both problems will be verified by the numerical experiments in next section.

3.1. Convergence results. In order to state the results, the following assumptions are firstly introduced:

- (I). **Coefficients.** The matrix $\mathbf{a}(\mathbf{y})$ possesses symmetry, uniform coercivity, and boundedness, that is, there exist positive constants $a_{\min}, a_{\max} > 0$, such that $a_{\min} \leq \mathbf{a}(\mathbf{y}) \leq a_{\max}$. Moreover, the periodic coefficients satisfy

$$\mathbf{a}(\mathbf{y}), M_s(\mathbf{y}) \text{ and } \gamma(\mathbf{y}) \in C^2(Y).$$

Additionally, the auxiliary functions defined in (2.12) and (2.22) satisfy

$$\chi(\mathbf{y}), U^*(\mathbf{y}), \theta(\mathbf{y}), \Lambda(\mathbf{y}) \text{ and } \rho(\mathbf{y}) \in C^2(Y).$$

For simplicity, the constant C_{coe} denotes the shared $C^2(Y)$ upper bound of the above periodic coefficients and auxiliary functions.

(II). **Initial data.** The initial data $\mathbf{m}_{\text{init}}^0(\mathbf{x}) \in C^4(\bar{\Omega})$ and $\mathbf{m}_{\text{init}}^\varepsilon(\mathbf{x}) \in C^2(\Omega)$ satisfy (2.31). Moreover, the following estimate holds

$$\|\mathbf{m}_{\text{init}}^\varepsilon(\mathbf{x}) - (\mathbf{m}_{\text{init}}^0(\mathbf{x}) + \tilde{\mathbf{m}}_{\text{init}}^c(\mathbf{x}))\|_{H^1(\Omega)} \leq C_{\text{coe}}\varepsilon.$$

Here, corrector $\tilde{\mathbf{m}}_{\text{init}}^c(\mathbf{x})$ is defined in (2.36), and $\mathbf{m}_{\text{init}}^0(\mathbf{x})$ is bounded by

$$\|\mathbf{m}_{\text{init}}^0\|_{C^4(\bar{\Omega})} \leq C_{\text{coe}}.$$

(III). **Boundary.** For the Neumann problem on the open bounded domain Ω , the boundary $\partial\Omega$ satisfies $\partial\Omega \in C^{1,1}$.

3.1.1. Periodic problem. The theoretical results for the Periodic problem are given as follows

THEOREM 3.1. *Let $\mathbf{m}^\varepsilon \in L^\infty(0, T; H^2(\Omega))$ be the unique solution of the multiscale LLG equation (2.24) and $\mathbf{m}_0 \in L^\infty(0, T; H^6(\Omega))$ be the unique solutions of the homogenized LLG equation (2.25), respectively. When $n = 3$, there exists some $T^* \in (0, T]$ independent of ε , such that for any $t \in (0, T^*)$, it holds*

$$(3.1) \quad \begin{aligned} & \|\mathbf{m}^\varepsilon(\mathbf{x}, t) - \mathbf{m}_0(\mathbf{x}, t)\|_{L^2(\Omega)} \leq C\varepsilon^{\frac{5}{6}} \ln(\varepsilon^{-1} + 1), \\ & \left\| \mathbf{m}^\varepsilon(\mathbf{x}, t) - \mathbf{m}_0(\mathbf{x}, t) - \varepsilon\chi\left(\frac{\mathbf{x}}{\varepsilon}\right) \nabla \mathbf{m}_0(\mathbf{x}, t) \right\|_{H^1(\Omega)} \leq C\varepsilon^{\frac{1}{2}} \ln(\varepsilon^{-1} + 1). \end{aligned}$$

Furthermore, when $n = 2$, there exists some $T^{**} \in (0, T]$ independent of ε , such that for any $t \in (0, T^{**})$, it holds

$$(3.2) \quad \begin{aligned} & \|\mathbf{m}^\varepsilon(\mathbf{x}, t) - \mathbf{m}_0(\mathbf{x}, t)\|_{L^2(\Omega)} \leq C\varepsilon^1, \\ & \left\| \mathbf{m}^\varepsilon(\mathbf{x}, t) - \mathbf{m}_0(\mathbf{x}, t) - \varepsilon\chi\left(\frac{\mathbf{x}}{\varepsilon}\right) \nabla \mathbf{m}_0(\mathbf{x}, t) \right\|_{H^1(\Omega)} \leq C\varepsilon^1. \end{aligned}$$

In both case, the constant C depends on C_{coe} , a_{\min} and a_{\max} given in Assumptions (I)-(II), but is independent of ε .

3.1.2. Neumann problem. For the Neumann problem, the Neumann corrector $\Phi^\varepsilon = \{\Phi_i^\varepsilon\}_{i=1}^n$ defined in (2.29) is employed to avoid the convergence deterioration on the boundary.

PROPOSITION 3.2. *Let $\mathbf{m}^\varepsilon \in L^\infty(0, T; H^2(\Omega))$ be the unique solution of the multiscale LLG equation (2.27) and $\mathbf{m}_0 \in L^\infty(0, T; H^6(\Omega))$ be the unique solutions of the homogenized LLG equation (2.28), respectively. When $n = 3$, there exists some $T^* \in (0, T]$ independent of ε , such that for any $t \in (0, T^*)$, it holds*

$$\begin{aligned} & \|\mathbf{m}^\varepsilon(\mathbf{x}, t) - \mathbf{m}_0(\mathbf{x}, t)\|_{L^2(\Omega)} \leq C\varepsilon^{\frac{5}{6}} \ln(\varepsilon^{-1} + 1), \\ & \|\mathbf{m}^\varepsilon(\mathbf{x}, t) - \mathbf{m}_0(\mathbf{x}, t) - (\Phi^\varepsilon - \mathbf{x}) \nabla \mathbf{m}_0(\mathbf{x}, t)\|_{H^1(\Omega)} \leq C\varepsilon^{\frac{1}{2}} \ln(\varepsilon^{-1} + 1). \end{aligned}$$

Furthermore, when $n = 2$, there exists some $T^{**} \in (0, T]$ independent of ε , such that for any $t \in (0, T^{**})$, it holds

$$\begin{aligned} & \|\mathbf{m}^\varepsilon(\mathbf{x}, t) - \mathbf{m}_0(\mathbf{x}, t)\|_{L^2(\Omega)} \leq C\varepsilon^1, \\ & \|\mathbf{m}^\varepsilon(\mathbf{x}, t) - \mathbf{m}_0(\mathbf{x}, t) - (\Phi^\varepsilon - \mathbf{x}) \nabla \mathbf{m}_0(\mathbf{x}, t)\|_{H^1(\Omega)} \leq C\varepsilon^1. \end{aligned}$$

In both case, the constant C depends on C_{coe} , a_{\min} and a_{\max} given in Assumptions (I)-(II), but is independent of ε .

It is worth noting that a multiscale elliptic problem with natural boundary conditions about Φ^ε is given in (2.29). Moreover, the spatial variable \mathbf{x} can be seen as the homogenized solution of this problem. By employing the elliptic homogenization theory, as outlined in Theorems 3.3.5 and 3.5.3 of [27], the following inequality can be obtained

$$(3.3) \quad \left\| \Phi^\varepsilon(\mathbf{x}) - \mathbf{x} - \varepsilon \chi \left(\frac{\mathbf{x}}{\varepsilon} \right) \right\|_{H^1(\Omega)} \leq C\varepsilon^{1/2}.$$

Substituting (3.3) into Theorem 3.2, the following proposition can be derived.

PROPOSITION 3.3. *Under the condition in Theorem 3.2, when $n = 3$, there exists some $T^* \in (0, T]$ independent of ε , such that for any $t \in (0, T^*)$, it holds*

$$\left\| \mathbf{m}^\varepsilon(\mathbf{x}, t) - \mathbf{m}_0(\mathbf{x}, t) - \varepsilon \chi \left(\frac{\mathbf{x}}{\varepsilon} \right) \nabla \mathbf{m}_0(\mathbf{x}, t) \right\|_{H^1(\Omega)} \leq C\varepsilon^{\frac{1}{2}} \ln(\varepsilon^{-1} + 1).$$

Furthermore, when $n = 2$, there exists some $T^{**} \in (0, T]$ independent of ε , such that for any $t \in (0, T^{**})$, it holds

$$\left\| \mathbf{m}^\varepsilon(\mathbf{x}, t) - \mathbf{m}_0(\mathbf{x}, t) - \varepsilon \chi \left(\frac{\mathbf{x}}{\varepsilon} \right) \nabla \mathbf{m}_0(\mathbf{x}, t) \right\|_{H^1(\Omega)} \leq C\varepsilon^{1/2}.$$

In both case, the constant C depends on C_{coe}, a_{\min} and a_{\max} given in Assumptions (I)-(II), but is independent of ε .

When employing the classical two-scale approximation to the multiscale LLG equation (2.27) under Neumann boundary condition, the convergence near the boundary will exhibit a degradation and a 1/2-order loss of convergence order. The detailed proof of the above propositions can refer to [10].

Remark 3.4. Comparing (3.1) with (3.2), it can be found that there are 1/6-order loss in the L^2 norm and 1/2-order loss in the H^1 norm. This degradation of convergence order is caused by boundary layer effects resulting from the zero extension of the stray fields (2.2).

Specifically, Table 2 presents the convergence orders of the 2D problems (2.24), (2.27) with the exchange field and degenerated stray field, where the two-scale corrector and the Neumann corrector are employed.

Boundary Condition	Approximation	Norm	Convergence Order
Periodic	$\mathbf{m}_0(\mathbf{x}) + \varepsilon \chi(\mathbf{x}/\varepsilon) \nabla \mathbf{m}_0(\mathbf{x})$	$L^2(\Omega)$	$\mathcal{O}(\varepsilon)$ [20]
		$H^1(\Omega)$	$\mathcal{O}(\varepsilon)$ (this work)
Neumann	$\mathbf{m}_0(\mathbf{x}) + (\Phi^\varepsilon(\mathbf{x}) - \mathbf{x}) \nabla \mathbf{m}_0(\mathbf{x})$	$L^2(\Omega)$	$\mathcal{O}(\varepsilon^{1/2})$ [10]
		$H^1(\Omega)$	$\mathcal{O}(\varepsilon)$ [10]

Table 2: Demonstration of convergence order for the 2D problem with the exchange field and degenerated stray field.

Remark 3.5. In Theorem 3.1, by choosing the correctors satisfying specific geometric property (2.7), the results (3.2) show that the approximation (1.2) has the

same convergence order in L^2 and H^1 norm. Here, the result in L_2 norm of (3.2) is consistent with the result of [20], but only the uniform boundedness in H^1 norm has been obtained in [20].

3.2. Proof of Theorem 3.1. The following proof is inspired by the Lax equivalence theorem [19]. For the 3D case, the LLG operator is defined as

$$(3.4) \quad \begin{cases} \mathcal{L}_{\text{LLG}}(\mathbf{m}^\varepsilon, U^\varepsilon) := \partial_t \mathbf{m}^\varepsilon - \alpha \mathcal{H}_e^\varepsilon(\mathbf{m}^\varepsilon, U^\varepsilon) + \mathbf{m}^\varepsilon \times \mathcal{H}_e^\varepsilon(\mathbf{m}^\varepsilon, U^\varepsilon) - \alpha g_l^\varepsilon(\mathbf{m}^\varepsilon, U^\varepsilon) \mathbf{m}^\varepsilon, \\ \mathcal{L}_{\text{SF}}(\mathbf{m}^\varepsilon, U^\varepsilon) := \Delta U^\varepsilon + \operatorname{div}(M^\varepsilon \mathbf{m}^\varepsilon \mathcal{X}_\Omega), \quad \text{in } D'(\mathbb{R}^3), \end{cases}$$

where the effective field $\mathcal{H}_e^\varepsilon$ takes the following form

$$(3.5) \quad \mathcal{H}_e^\varepsilon(\mathbf{m}^\varepsilon, U^\varepsilon) = \operatorname{div}(\mathbf{a}^\varepsilon \nabla \mathbf{m}^\varepsilon) - K^\varepsilon (\mathbf{m}^\varepsilon \cdot \mathbf{u}) \mathbf{u} + M^\varepsilon \mathbf{h}_a + \mu^\varepsilon \nabla U^\varepsilon,$$

and the $g_l^\varepsilon[\cdot]$ is the energy density calculated by

$$(3.6) \quad g_l^\varepsilon(\mathbf{m}^\varepsilon, U^\varepsilon) = \mathbf{a}^\varepsilon |\nabla \mathbf{m}^\varepsilon|^2 + K^\varepsilon (\mathbf{m}^\varepsilon \cdot \mathbf{u})^2 - \mu^\varepsilon \nabla U^\varepsilon \cdot M^\varepsilon \mathbf{m}^\varepsilon - \mathbf{h}_a \cdot M^\varepsilon \mathbf{m}^\varepsilon.$$

The classical solution \mathbf{m}^ε of (2.5) with the stray field U^ε satisfies

$$(3.7) \quad \mathcal{L}_{\text{LLG}}(\mathbf{m}^\varepsilon, U^\varepsilon) = 0, \quad \mathcal{L}_{\text{SF}}(\mathbf{m}^\varepsilon, U^\varepsilon) = 0.$$

With the two-scale approximation $\tilde{\mathbf{m}}^\varepsilon$ and \tilde{U}^ε defined in (2.6), the approximate stray field Γ^ε induced by $\tilde{\mathbf{m}}^\varepsilon$ can be defined as

$$(3.8) \quad \mathcal{L}_{\text{SF}}(\tilde{\mathbf{m}}^\varepsilon, \Gamma^\varepsilon) = 0.$$

Then, the consistency error $\Theta_{\text{total}}^\varepsilon$ is decomposed into two parts

$$(3.9) \quad \begin{aligned} \Theta_{\text{total}}^\varepsilon &:= \mathcal{L}_{\text{LLG}}(\tilde{\mathbf{m}}^\varepsilon, \Gamma^\varepsilon) \\ &= \mathcal{L}_{\text{LLG}}(\tilde{\mathbf{m}}^\varepsilon, \tilde{U}^\varepsilon) + \{ \mathcal{L}_{\text{LLG}}(\tilde{\mathbf{m}}^\varepsilon, \Gamma^\varepsilon) - \mathcal{L}_{\text{LLG}}(\tilde{\mathbf{m}}^\varepsilon, \tilde{U}^\varepsilon) \} \\ &=: \Theta_{\text{ts}}^\varepsilon + \Theta_{\text{sf}}^\varepsilon. \end{aligned}$$

where $\Theta_{\text{ts}}^\varepsilon$ is induced by the two-scale approximation, and $\Theta_{\text{sf}}^\varepsilon$ is induced by the stray field.

On the other hand, the error $\mathbf{e}^\varepsilon(\mathbf{x})$ and $\Psi^\varepsilon(\mathbf{x})$ between the classical solution and the approximating solution is defined as

$$(3.10) \quad \mathbf{m}^\varepsilon(\mathbf{x}) = \tilde{\mathbf{m}}^\varepsilon(\mathbf{x}) + \mathbf{e}^\varepsilon(\mathbf{x}), \quad U^\varepsilon(\mathbf{x}) = \Gamma^\varepsilon(\mathbf{x}) + \Psi^\varepsilon(\mathbf{x}).$$

By subtracting (3.9) from (3.7), the equation about \mathbf{e}^ε and Ψ^ε is given by

$$(3.11) \quad \begin{cases} \partial_t \mathbf{e}^\varepsilon - \alpha \tilde{\mathcal{H}}_e^\varepsilon(\mathbf{e}^\varepsilon, \Psi^\varepsilon) - \mathbf{D}_1(\mathbf{e}^\varepsilon, \Psi^\varepsilon) - \mathbf{D}_2(\mathbf{e}^\varepsilon, \Psi^\varepsilon) = -(\Theta_{\text{ts}}^\varepsilon + \Theta_{\text{sf}}^\varepsilon), \\ \mathcal{L}_{\text{SF}}(\mathbf{e}^\varepsilon, \Psi^\varepsilon) = 0. \end{cases}$$

Here, $\tilde{\mathcal{H}}_e^\varepsilon$ is the linear part of $\mathcal{H}_e^\varepsilon$, i.e.,

$$\tilde{\mathcal{H}}_e^\varepsilon(\mathbf{e}^\varepsilon, \Psi^\varepsilon) := \mathcal{H}_e^\varepsilon(\mathbf{e}^\varepsilon, \Psi^\varepsilon) - M^\varepsilon \mathbf{h}_a.$$

The precession term \mathbf{D}_1 is calculated by

$$(3.12) \quad \begin{aligned} \mathbf{D}_1(\mathbf{e}^\varepsilon, \Psi^\varepsilon) &= \mathbf{m}^\varepsilon \times \mathcal{H}_e^\varepsilon(\mathbf{m}^\varepsilon, U^\varepsilon) - \tilde{\mathbf{m}}^\varepsilon \times \mathcal{H}_e^\varepsilon(\tilde{\mathbf{m}}^\varepsilon, \Gamma^\varepsilon) \\ &= \mathbf{m}^\varepsilon \times \tilde{\mathcal{H}}_e^\varepsilon(\mathbf{e}^\varepsilon, \Psi^\varepsilon) + \mathbf{e}^\varepsilon \times \mathcal{H}_e^\varepsilon(\tilde{\mathbf{m}}^\varepsilon, \Gamma^\varepsilon), \end{aligned}$$

and the degeneracy term \mathbf{D}_2 reads as

$$\begin{aligned}\mathbf{D}_2(\mathbf{e}^\varepsilon, \Psi^\varepsilon) &= -\alpha g_l^\varepsilon(\mathbf{m}^\varepsilon, U^\varepsilon)\mathbf{m}^\varepsilon + \alpha g_l^\varepsilon(\tilde{\mathbf{m}}^\varepsilon, \Gamma^\varepsilon)\tilde{\mathbf{m}}^\varepsilon \\ &= -\alpha(\nabla \mathbf{e}^\varepsilon \cdot \mathbf{a}^\varepsilon \nabla \mathbf{m}^\varepsilon + \nabla \mathbf{e}^\varepsilon \cdot \mathbf{a}^\varepsilon \nabla \tilde{\mathbf{m}}^\varepsilon)\mathbf{m}^\varepsilon \\ &\quad -\alpha(K^\varepsilon(\mathbf{m}^\varepsilon \cdot \mathbf{u})(\mathbf{e}^\varepsilon \cdot \mathbf{u}) + K^\varepsilon(\tilde{\mathbf{m}}^\varepsilon \cdot \mathbf{u})(\mathbf{e}^\varepsilon \cdot \mathbf{u}))\mathbf{m}^\varepsilon \\ &\quad -\alpha(\mu^\varepsilon \nabla U^\varepsilon \cdot \mathbf{e}^\varepsilon + \mu^\varepsilon \nabla \Gamma^\varepsilon \cdot \tilde{\mathbf{m}}^\varepsilon + M^\varepsilon(\mathbf{h}_a \cdot \mathbf{e}^\varepsilon))\mathbf{m}^\varepsilon - \alpha g_l^\varepsilon(\tilde{\mathbf{m}}^\varepsilon, \Gamma^\varepsilon)\mathbf{e}^\varepsilon.\end{aligned}$$

By employing the idea of Lax equivalence theorem, the estimate of errors \mathbf{e}^ε and Ψ^ε can be derived by two steps: the consistency analysis of (3.9), and the stability analysis of (3.11).

Firstly, the result of consistency analysis is given in the following lemma.

LEMMA 3.6. *Suppose Assumptions (I)-(II) hold. For the consistency error $\Theta_{\text{total}}^\varepsilon = \Theta_{\text{ts}}^\varepsilon + \Theta_{\text{sf}}^\varepsilon$ given in (3.9), it holds*

$$\begin{aligned}\|\Theta_{\text{ts}}^\varepsilon(\mathbf{x})\|_{L^2(\Omega)} &\leq C\varepsilon, \\ \|\Theta_{\text{sf}}^\varepsilon\|_{L^r(\Omega)} &\leq C_r \varepsilon^{1/r} \ln(\varepsilon^{-1} + 1),\end{aligned}$$

for any $1 < r < \infty$. Here, the constants C and C_r depend on C_{coe} and $\|\mathbf{m}_0\|_{W^{4,\infty}(\Omega)}$, but are independent of ε .

Secondly, the results of stability analysis are presented in Lemma 3.7 and Lemma 3.8.

LEMMA 3.7. *Let $\mathbf{e}^\varepsilon \in L^\infty(0, T; H^2(\Omega))$ be a strong solution to (3.11). Suppose Assumptions (I)-(II) hold. For the 3D case, it holds*

$$(3.13) \quad \|\mathbf{e}^\varepsilon\|_{L^\infty(0, T; L^2(\Omega))}^2 \leq C(\|\mathbf{e}^\varepsilon(\mathbf{x}, 0)\|_{L^2(\Omega)}^2 + \|\Theta_{\text{ts}}^\varepsilon\|_{L^2(0, T; L^2(\Omega))}^2 + \|\Theta_{\text{sf}}^\varepsilon\|_{L^2(0, T; L^{6/5}(\Omega))}^2),$$

and

$$(3.14) \quad \|\nabla \mathbf{e}^\varepsilon\|_{L^\infty(0, T; L^2(\Omega))}^2 \leq C(\|\mathbf{e}^\varepsilon(\mathbf{x}, 0)\|_{H^1(\Omega)}^2 + \|\Theta_{\text{ts}}^\varepsilon\|_{L^2(0, T; L^2(\Omega))}^2 + \|\Theta_{\text{sf}}^\varepsilon\|_{L^2(0, T; L^2(\Omega))}^2),$$

where the constant C depends on C_{coe} , $\|\mathbf{m}_0\|_{W^{4,\infty}(\Omega)}$ and $\|\nabla \mathbf{m}^\varepsilon\|_{L^6(\Omega)}$.

Together with Lemma 3.6 and Lemma 3.7, the estimate of $\|\mathbf{e}^\varepsilon\|_{L^\infty(0, T; L^2(\Omega))}^2$ and $\|\nabla \mathbf{e}^\varepsilon\|_{L^\infty(0, T; L^2(\Omega))}^2$ can be obtained with Grönwall's inequality:

$$(3.15) \quad \begin{aligned}\|\mathbf{e}^\varepsilon(\cdot, t)\|_{L^\infty(0, T; L^2(\Omega))} &\leq C(\|\nabla \mathbf{m}^\varepsilon\|_{L^6(\Omega)}) \varepsilon^{5/6} \ln(\varepsilon^{-1} + 1), \\ \|\mathbf{e}^\varepsilon(\cdot, t)\|_{L^\infty(0, T; H^1(\Omega))} &\leq C(\|\nabla \mathbf{m}^\varepsilon\|_{L^6(\Omega)}) \varepsilon^{1/2} \ln(\varepsilon^{-1} + 1).\end{aligned}$$

However, the above constants depend on the bound of $\|\nabla \mathbf{m}^\varepsilon\|_{L^6(\Omega)}$. In order to derive an ε -independent estimate, the following lemma is introduced.

LEMMA 3.8. *Under Assumptions (I)-(II), there exists $T^* \in (0, T]$ independent of ε , such that for $0 \leq t \leq T^*$,*

$$\|\nabla \mathbf{m}^\varepsilon(\cdot, t)\|_{L^6(\Omega)}^2 \leq C,$$

where the constant C depends on C_{coe} , a_{min} and a_{max} , but is independent of ε and t .

Remark 3.9. Comparing with the similar results in [10], the more complex lower-order terms are considered in our multiscale LLG model. The proof of Lemma 3.6, Lemma 3.7, and Lemma 3.8 can be found in Appendix A, Appendix B, and Appendix C, respectively.

Utilizing (3.15) and Lemma 3.8, one can derive that for some $0 < T^* \leq T$, it holds

$$(3.16) \quad \begin{aligned} \|\mathbf{e}^\varepsilon(\cdot, t)\|_{L^\infty(0, T^*; L^2(\Omega))} &\leq C\varepsilon^{5/6} \ln(\varepsilon^{-1} + 1), \\ \|\mathbf{e}^\varepsilon(\cdot, t)\|_{L^\infty(0, T^*; H^1(\Omega))} &\leq C\varepsilon^{1/2} \ln(\varepsilon^{-1} + 1). \end{aligned}$$

Here, the constant C depends on C_{coe} , a_{\min} and a_{\max} , but is independent of ε . Moreover, revisit the definition of $\mathbf{e}^\varepsilon(\mathbf{x})$ in (3.10), we have

$$(3.17) \quad \mathbf{e}^\varepsilon(\mathbf{x}) = \mathbf{m}^\varepsilon(\mathbf{x}) - \mathbf{m}_0(\mathbf{x}) - \varepsilon \mathbf{m}_1\left(\mathbf{x}, \frac{\mathbf{x}}{\varepsilon}\right) - \varepsilon^2 \mathbf{m}_2\left(\mathbf{x}, \frac{\mathbf{x}}{\varepsilon}\right).$$

Based on the definition of \mathbf{m}_2 in (2.21) and Assumption (I), there exists some constant C independent of ε , such that

$$(3.18) \quad \varepsilon^2 \left\| \mathbf{m}_2\left(\mathbf{x}, \frac{\mathbf{x}}{\varepsilon}\right) \right\|_{H^1(\Omega)} \leq \varepsilon \|\mathbf{m}_2(\mathbf{x}, \mathbf{y})\|_{W^{1, \infty}(\Omega \times Y)} \leq C\varepsilon.$$

For the 3D case, combining (3.16), (3.17) with (3.18), the estimates (3.1) in Theorem 3.1 can be derived.

For the 2D case, the stray field degenerates to a simple form (2.3), and the error $\Theta_{\text{sf}}^\varepsilon$ disappears. Therefore, by setting $\Theta_{\text{sf}}^\varepsilon = 0$, one can prove that Lemma 3.6, Lemma 3.7 and Lemma 3.8 still hold. Finally, the 2D part of Theorem 3.1 can be similarly deduced. The proof is completed.

4. Numerical experiments. This section provides several numerical examples to verify the convergence results presented in section 3. Moreover, it demonstrates the proposed framework's robustness in simulating the multiscale LLG equation under different boundary conditions and effective fields. To simplify the representation of approximate error in Theorem 3.1 and Proposition 3.2, the following notations are introduced.

$$(4.1) \quad \begin{aligned} e_0 &= \|\mathbf{m}^\varepsilon(\mathbf{x}, t) - \mathbf{m}_0(\mathbf{x}, t)\|_{L^2(\Omega)}, \quad \tilde{e}_0 = e_0 / \|\mathbf{m}^\varepsilon(\mathbf{x}, t)\|_{L^2(\Omega)}, \\ e_1 &= \left\| \mathbf{m}^\varepsilon(\mathbf{x}, t) - \mathbf{m}_0(\mathbf{x}, t) - \varepsilon \chi\left(\frac{\mathbf{x}}{\varepsilon}\right) \nabla \mathbf{m}_0(\mathbf{x}, t) \right\|_{H^1(\Omega)}, \quad \tilde{e}_1 = e_1 / \|\mathbf{m}^\varepsilon(\mathbf{x}, t)\|_{H^1(\Omega)}, \\ e_2 &= \|\mathbf{m}^\varepsilon(\mathbf{x}, t) - \mathbf{m}_0(\mathbf{x}, t) - (\Phi^\varepsilon - \mathbf{x}) \nabla \mathbf{m}_0(\mathbf{x}, t)\|_{H^1(\Omega)}, \quad \tilde{e}_2 = e_2 / \|\mathbf{m}^\varepsilon(\mathbf{x}, t)\|_{H^1(\Omega)}. \end{aligned}$$

For the 2D examples, the problems (1.1) are considered in the domain $\Omega = [0, 1]^2$. The finite element solutions with spatial mesh size $h = 1/180$ are employed as the reference. The reference solutions and the homogenized solutions share the consistent time step size $\Delta t = 10^{-6}$ and damping constant $\alpha = 1$. The initial data $\mathbf{m}_{\text{init}}^0(\mathbf{x})$ of the homogenized system is defined as

$$\mathbf{m}_{\text{init}}^0(\mathbf{x}) = \begin{cases} (0, 0, -1) & \text{for } |\tilde{\mathbf{x}}| \geq 1/2 \\ (2\tilde{x}_1 A, 2\tilde{x}_2 A, A^2 - |\tilde{\mathbf{x}}|^2) / (A^2 + |\tilde{\mathbf{x}}|^2) & \text{for } |\tilde{\mathbf{x}}| \leq 1/2 \end{cases},$$

where $\tilde{\mathbf{x}} = (\tilde{x}_1, \tilde{x}_2) = (x_1 - 1/2, x_2 - 1/2)$, and $A := (1 - 2|\tilde{\mathbf{x}}|)^4$.

4.1. 2D Periodic problem. This example presents the simulation results for the 2D Periodic problem involving the exchange field. The exchange field is the second-order term of the effective field and plays a dominant role in the evolution of

the multiscale LLG system. In this case, the multiscale LLG equation is given by

$$\begin{cases} \partial_t \mathbf{m}^\varepsilon - \alpha \mathbf{m}^\varepsilon \times \partial_t \mathbf{m}^\varepsilon = - (1 + \alpha^2) \mathbf{m}^\varepsilon \times \operatorname{div} (\mathbf{a}^\varepsilon \nabla \mathbf{m}^\varepsilon) & \text{in } \Omega, \\ \mathbf{m}^\varepsilon(\mathbf{x}, 0) = \mathbf{m}_{\text{init}}^\varepsilon(\mathbf{x}), \quad |\mathbf{m}_{\text{init}}^\varepsilon(\mathbf{x})| = 1 & \text{in } \Omega, \\ \mathbf{m}^\varepsilon(\mathbf{x}, t), \mathbf{m}_{\text{init}}^\varepsilon(\mathbf{x}) & \text{are periodic on } \partial\Omega. \end{cases}$$

The corresponding homogenized LLG equation is

$$\begin{cases} \partial_t \mathbf{m}_0 - \alpha \mathbf{m}_0 \times \partial_t \mathbf{m}_0 = - (1 + \alpha^2) \mathbf{m}_0 \times \operatorname{div} (\mathbf{a}^0 \nabla \mathbf{m}_0) & \text{in } \Omega, \\ \mathbf{m}_0(\mathbf{x}, 0) = \mathbf{m}_{\text{init}}^0(\mathbf{x}), \quad |\mathbf{m}_{\text{init}}^0(\mathbf{x})| = 1 & \text{in } \Omega, \\ \mathbf{m}_0(\mathbf{x}, t), \mathbf{m}_{\text{init}}^0(\mathbf{x}) & \text{are periodic on } \partial\Omega. \end{cases}$$

The initial data of the multiscale LLG equation is obtained by the expansion method

$$\mathbf{m}_{\text{init}}^\varepsilon(\mathbf{x}) = \mathbf{m}_{\text{init}}^0(\mathbf{x}) + \varepsilon \chi \left(\frac{\mathbf{x}}{\varepsilon} \right) \nabla \mathbf{m}_{\text{init}}^0(\mathbf{x}).$$

For the 2D Periodic problem only with the exchange field, the convergence results are given as follows

$$\begin{aligned} \|\mathbf{m}^\varepsilon(\mathbf{x}, t) - \mathbf{m}_0(\mathbf{x}, t)\|_{L^2(\Omega)} &\leq C\varepsilon^1, \\ \left\| \mathbf{m}^\varepsilon(\mathbf{x}, t) - \mathbf{m}_0(\mathbf{x}, t) - \varepsilon \chi \left(\frac{\mathbf{x}}{\varepsilon} \right) \nabla \mathbf{m}_0(\mathbf{x}, t) \right\|_{H^1(\Omega)} &\leq C\varepsilon^1. \end{aligned}$$

Under assumption (2.4), the exchange coefficient \mathbf{a}^ε can be defined by $\mathbf{a}(\mathbf{y})$

$$\mathbf{a}(\mathbf{y}) = \left(1.1 + 0.25 \cos(2\pi(y_1 - 0.5)) \right) \left(1.1 + 0.25 \cos(2\pi(y_2 - 0.5)) \right) \times I_2,$$

where I_2 is the 2×2 identity matrix.

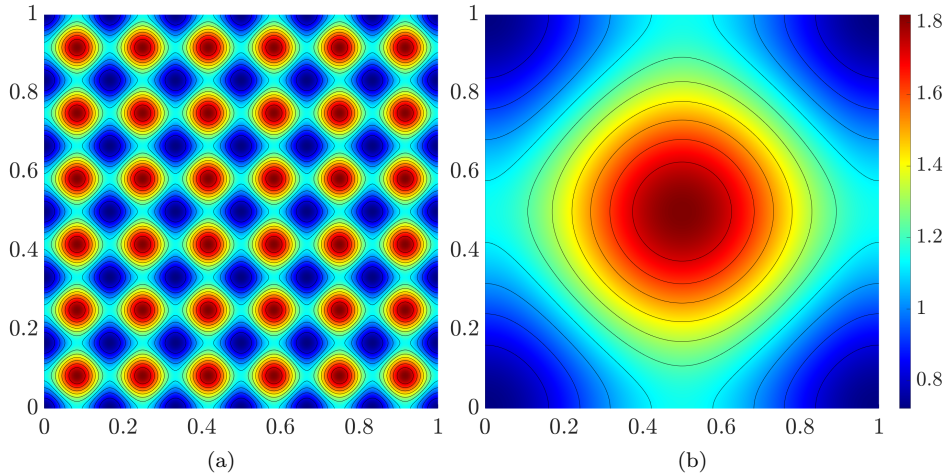


Fig. 1: Multiscale exchange coefficient $\mathbf{a}^\varepsilon(\mathbf{x})$ defined in (a) the whole computational domain Ω , and (b) the reference unit cell Y .

Figure 2 shows two auxiliary functions χ_1 and χ_2 of the first-order cell problem

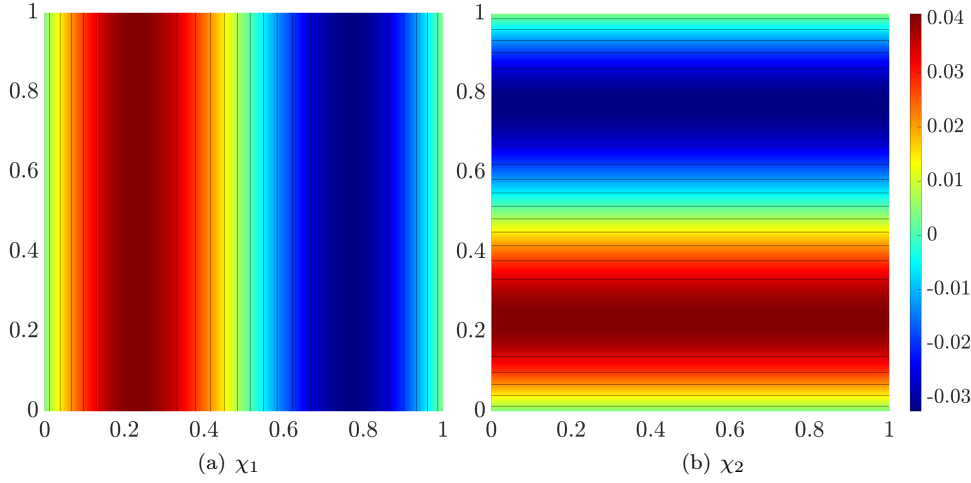


Fig. 2: Demonstration of the auxiliary functions χ_1, χ_2 .

(2.12), which are utilized to obtain the corresponding homogenized coefficients \mathbf{a}^0 by (2.17).

$$\mathbf{a}^0 = \begin{pmatrix} 1.178 & 1.073 \times 10^{-9} \\ 1.073 \times 10^{-9} & 1.178 \end{pmatrix}.$$

Table 3 presents the error results at different time $t = j\Delta t$ with various numbers of periods n , where the corresponding error convergence orders are depicted in Figure 3. From the figure, the error convergence orders obtained from the proposed framework is consistent with the theoretical results. As time increases, the computational errors inevitably accumulate, eventually leading to a slight decrease in the convergence order at $j = 10^3$.

n	j=10		j=10 ²		j=10 ³	
	e_0	\tilde{e}_0	e_0	\tilde{e}_0	e_0	\tilde{e}_0
2	1.18×10^{-1}	1.18×10^{-1}	1.17×10^{-1}	1.17×10^{-1}	1.09×10^{-1}	1.09×10^{-1}
3	6.34×10^{-2}	6.34×10^{-2}	6.26×10^{-2}	6.26×10^{-2}	5.81×10^{-2}	5.81×10^{-2}
4	4.46×10^{-2}	4.46×10^{-2}	4.45×10^{-2}	4.45×10^{-2}	4.52×10^{-2}	4.52×10^{-2}
5	3.77×10^{-2}	3.78×10^{-2}	3.76×10^{-2}	3.76×10^{-2}	3.91×10^{-2}	3.91×10^{-2}
6	3.25×10^{-2}	3.25×10^{-2}	3.21×10^{-2}	3.21×10^{-2}	3.27×10^{-2}	3.27×10^{-2}
	e_1	\tilde{e}_1	e_1	\tilde{e}_1	e_1	\tilde{e}_1
2	2.14	3.33×10^{-1}	2.06	3.23×10^{-1}	1.54	2.59×10^{-1}
3	1.13	1.55×10^{-1}	1.10	1.52×10^{-1}	9.38×10^{-1}	1.42×10^{-1}
4	7.94×10^{-1}	1.18×10^{-1}	7.76×10^{-1}	1.17×10^{-1}	7.05×10^{-1}	1.13×10^{-1}
5	6.72×10^{-1}	9.94×10^{-2}	6.57×10^{-1}	9.80×10^{-2}	6.34×10^{-1}	1.01×10^{-1}
6	5.81×10^{-1}	8.35×10^{-2}	5.70×10^{-1}	8.28×10^{-2}	5.64×10^{-1}	8.87×10^{-2}

Table 3: Error of the 2D Periodic problem under various numbers of periods $n = 1/\varepsilon$ at time $t = j\Delta t$.

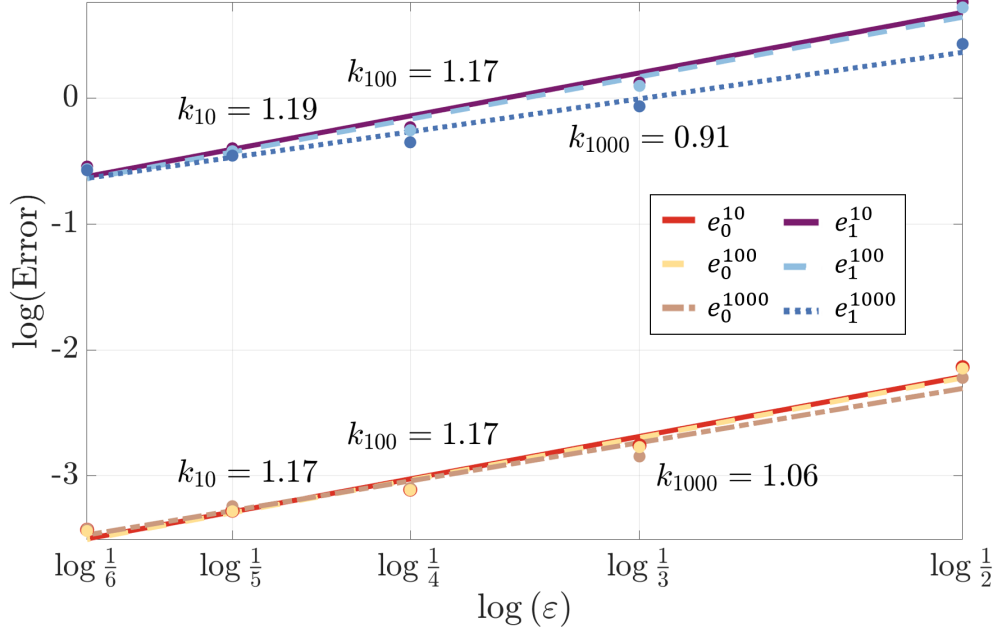


Fig. 3: Variation of error e_0^j and e_1^j relative to the cell size ε across different time steps j in the 2D Periodic problem.

4.2. 2D Neumann problem. For the Neumann problem, the effective field $\mathbf{h}_{\text{eff}}^\varepsilon$ and the multiscale exchange coefficient \mathbf{a}^ε are considered with the same situation of subsection 4.1. In this case, the multiscale LLG equation is expressed as

$$\begin{cases} \partial_t \mathbf{m}^\varepsilon - \alpha \mathbf{m}^\varepsilon \times \partial_t \mathbf{m}^\varepsilon = - (1 + \alpha^2) \mathbf{m}^\varepsilon \times \text{div} (\mathbf{a}^\varepsilon \nabla \mathbf{m}^\varepsilon) & \text{in } \Omega, \\ \mathbf{m}^\varepsilon(\mathbf{x}, 0) = \mathbf{m}_{\text{init}}^\varepsilon(\mathbf{x}), \quad |\mathbf{m}_{\text{init}}^\varepsilon(\mathbf{x})| = 1 & \text{in } \Omega, \\ \boldsymbol{\nu} \cdot \mathbf{a}^\varepsilon \nabla \mathbf{m}^\varepsilon(\mathbf{x}, t) = 0, & \text{on } \partial\Omega \times [0, T], \\ \boldsymbol{\nu} \cdot \mathbf{a}^\varepsilon \nabla \mathbf{m}_{\text{init}}^\varepsilon(\mathbf{x}) = 0, & \text{on } \partial\Omega. \end{cases}$$

The corresponding homogenized LLG equation is

$$\begin{cases} \partial_t \mathbf{m}_0 - \alpha \mathbf{m}_0 \times \partial_t \mathbf{m}_0 = - (1 + \alpha^2) \mathbf{m}_0 \times \text{div} (\mathbf{a}^0 \nabla \mathbf{m}_0) & \text{in } \Omega, \\ \mathbf{m}_0(\mathbf{x}, 0) = \mathbf{m}_{\text{init}}^0(\mathbf{x}), \quad |\mathbf{m}_{\text{init}}^0(\mathbf{x})| = 1 & \text{in } \Omega, \\ \boldsymbol{\nu} \cdot \mathbf{a}^0 \nabla \mathbf{m}_0(\mathbf{x}, t) = 0, & \text{on } \partial\Omega \times [0, T], \\ \boldsymbol{\nu} \cdot \mathbf{a}^0 \nabla \mathbf{m}_{\text{init}}^0(\mathbf{x}) = 0, & \text{on } \partial\Omega. \end{cases}$$

Here, we employ the expansion method to obtain the initial data of the multiscale LLG equation

$$\mathbf{m}_{\text{init}}^\varepsilon(\mathbf{x}) = \mathbf{m}_{\text{init}}^0(\mathbf{x}) + (\boldsymbol{\Phi}^\varepsilon - \mathbf{x}) \nabla \mathbf{m}_{\text{init}}^0(\mathbf{x}),$$

where $\boldsymbol{\Phi}^\varepsilon$ is the Neumann corrector defined in (2.29). For the 2D Neumann problem only with the exchange field, the convergence results are given as follows

$$\begin{aligned} \|\mathbf{m}^\varepsilon(\mathbf{x}, t) - \mathbf{m}_0(\mathbf{x}, t)\|_{L^2(\Omega)} &\leq C\varepsilon^1, \\ \|\mathbf{m}^\varepsilon(\mathbf{x}, t) - \mathbf{m}_0(\mathbf{x}, t) - (\boldsymbol{\Phi}^\varepsilon - \mathbf{x}) \nabla \mathbf{m}_0(\mathbf{x}, t)\|_{H^1(\Omega)} &\leq C\varepsilon^1. \end{aligned}$$

The error results of the Neumann problem are shown in Table 4. As depicted in Figure 4, the obtained convergence orders align well with theoretical results. The similar trends of convergence orders are observed for the Periodic problem and the Neumann problem.

n	$j=10$		$j=10^2$		$j=10^3$	
	e_0	\tilde{e}_0	e_0	\tilde{e}_0	e_0	\tilde{e}_0
2	1.13×10^{-1}	1.13×10^{-1}	1.13×10^{-1}	1.13×10^{-1}	1.05×10^{-1}	1.05×10^{-1}
3	5.80×10^{-2}	5.80×10^{-2}	5.72×10^{-2}	5.72×10^{-2}	5.30×10^{-2}	5.30×10^{-2}
4	4.01×10^{-2}	4.01×10^{-2}	4.00×10^{-2}	4.00×10^{-2}	4.14×10^{-2}	4.14×10^{-2}
5	3.42×10^{-2}	3.42×10^{-2}	3.41×10^{-2}	3.41×10^{-2}	3.63×10^{-2}	3.63×10^{-2}
6	2.96×10^{-2}	2.96×10^{-2}	2.93×10^{-2}	2.93×10^{-2}	3.03×10^{-2}	3.03×10^{-2}
	e_2	\tilde{e}_2	e_2	\tilde{e}_2	e_2	\tilde{e}_2
2	2.02	3.14×10^{-1}	1.93	3.04×10^{-1}	1.44	2.42×10^{-1}
3	1.03	1.41×10^{-1}	1.01	1.39×10^{-1}	8.71×10^{-1}	1.32×10^{-1}
4	7.18×10^{-1}	1.07×10^{-1}	7.02×10^{-1}	1.06×10^{-1}	6.57×10^{-1}	1.06×10^{-1}
5	6.07×10^{-1}	8.97×10^{-2}	5.94×10^{-1}	8.87×10^{-2}	5.97×10^{-1}	9.56×10^{-2}
6	5.27×10^{-1}	7.57×10^{-2}	5.18×10^{-1}	7.52×10^{-2}	5.35×10^{-1}	8.41×10^{-2}

Table 4: Error of the 2D Neumann problem under various numbers of periods $n = 1/\varepsilon$ at time $t = j\Delta t$.

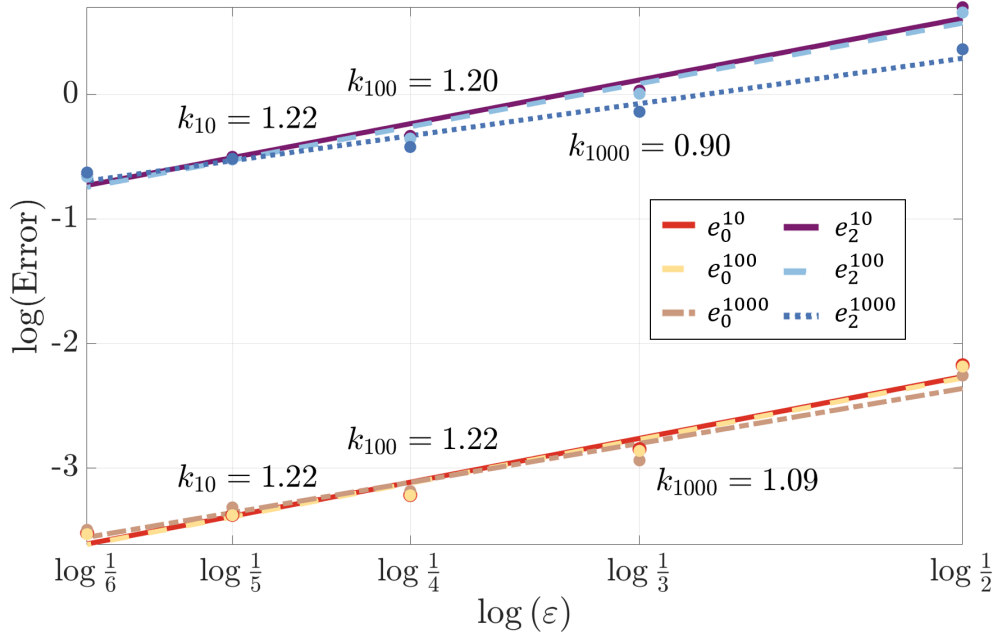


Fig. 4: Variation of error e_0^j and e_2^j relative to the cell size ε across different time steps j in the 2D Neumann problem.

4.3. 2D Periodic problem with degenerated stray field. The dominant exchange field is considered in previous two numerical experiments. However, the stray field also plays an important role in practical engineering, and numerical simulation of its corresponding potential function is challenging.

In this numerical experiment, we consider the Periodic problem involving the

exchange field and the stray field. For simplicity, the problem is restricted to the thin film materials. In this case, the stray field degenerates into a linear field, which can significantly decrease the complexity of the simulation. The multiscale LLG equation is given by

$$\begin{cases} \partial_t \mathbf{m}^\varepsilon - \alpha \mathbf{m}^\varepsilon \times \partial_t \mathbf{m}^\varepsilon = - (1 + \alpha^2) \mathbf{m}^\varepsilon \times [\operatorname{div}(\mathbf{a}^\varepsilon \nabla \mathbf{m}^\varepsilon) + \mu^\varepsilon (\mathbf{m}^\varepsilon \cdot \mathbf{e}_3) \mathbf{e}_3] & \text{in } \Omega, \\ \mathbf{m}^\varepsilon(\mathbf{x}, 0) = \mathbf{m}_{\text{init}}^\varepsilon(\mathbf{x}), \quad |\mathbf{m}_{\text{init}}^\varepsilon(\mathbf{x})| = 1 & \text{in } \Omega, \\ \mathbf{m}^\varepsilon(\mathbf{x}, t), \mathbf{m}_{\text{init}}^\varepsilon(\mathbf{x}) & \text{are periodic on } \partial\Omega. \end{cases}$$

The corresponding homogenized LLG equation can be expressed as

$$\begin{cases} \partial_t \mathbf{m}_0 - \alpha \mathbf{m}_0 \times \partial_t \mathbf{m}_0 = - (1 + \alpha^2) \mathbf{m}_0 \times [\operatorname{div}(\mathbf{a}^0 \nabla \mathbf{m}_0) + \mu^0 (\mathbf{m}_0 \cdot \mathbf{e}_3) \mathbf{e}_3] & \text{in } \Omega, \\ \mathbf{m}_0(\mathbf{x}, 0) = \mathbf{m}_{\text{init}}^0(\mathbf{x}), \quad |\mathbf{m}_{\text{init}}^0(\mathbf{x})| = 1 & \text{in } \Omega, \\ \mathbf{m}_0(\mathbf{x}, t), \mathbf{m}_{\text{init}}^0(\mathbf{x}) & \text{are periodic on } \partial\Omega. \end{cases}$$

Here, we also obtain the initial data of the multiscale LLG equation by the expansion method (2.35). For the Periodic problem involving the exchange field and the degenerated stray field, the theoretical results remain consistent with the case considering only the exchange field. This is because only a linear term is introduced into the effective field. The corresponding convergence results are given as follows

$$\begin{aligned} \|\mathbf{m}^\varepsilon(\mathbf{x}, t) - \mathbf{m}_0(\mathbf{x}, t)\|_{L^2(\Omega)} &\leq C\varepsilon^1, \\ \left\| \mathbf{m}^\varepsilon(\mathbf{x}, t) - \mathbf{m}_0(\mathbf{x}, t) - \varepsilon \chi\left(\frac{\mathbf{x}}{\varepsilon}\right) \nabla \mathbf{m}_0(\mathbf{x}, t) \right\|_{H^1(\Omega)} &\leq C\varepsilon^1. \end{aligned}$$

In this case, the positive multiscale coefficient μ^ε is defined by

$$\mu^\varepsilon(\mathbf{y}) = (1.1 + 0.25 \sin(2\pi y_1))(1.1 + 0.25 \sin(2\pi y_2)).$$

Moreover, the exchange coefficient \mathbf{a}^ε is consistent with subsection 4.1 and subsection 4.2. Then, Table 5 and Figure 5 present the error results. Considering the effect of stray field, we still obtain the computational results, which closely align with the theoretical results.

n	$j=10$		$j=10^2$		$j=10^3$	
	e_0	\tilde{e}_0	e_0	\tilde{e}_0	e_0	\tilde{e}_0
2	1.18×10^{-1}	1.18×10^{-1}	1.17×10^{-1}	1.17×10^{-1}	1.09×10^{-1}	1.09×10^{-1}
3	6.34×10^{-2}	6.34×10^{-2}	6.26×10^{-2}	6.26×10^{-2}	5.81×10^{-2}	5.81×10^{-2}
4	4.46×10^{-2}	4.46×10^{-2}	4.45×10^{-2}	4.45×10^{-2}	4.52×10^{-2}	4.52×10^{-2}
5	3.77×10^{-2}	3.78×10^{-2}	3.76×10^{-2}	3.76×10^{-2}	3.91×10^{-2}	3.91×10^{-2}
6	3.25×10^{-2}	3.25×10^{-2}	3.21×10^{-2}	3.21×10^{-2}	3.26×10^{-2}	3.27×10^{-2}
	e_1	\tilde{e}_1	e_1	\tilde{e}_1	e_1	\tilde{e}_1
2	2.14	3.33×10^{-1}	2.06	3.23×10^{-1}	1.54	2.58×10^{-1}
3	1.13	1.55×10^{-1}	1.10	1.52×10^{-1}	9.37×10^{-1}	1.42×10^{-1}
4	7.94×10^{-1}	1.18×10^{-1}	7.76×10^{-1}	1.17×10^{-1}	7.05×10^{-1}	1.13×10^{-1}
5	6.72×10^{-1}	9.94×10^{-2}	6.57×10^{-1}	9.80×10^{-2}	6.34×10^{-1}	1.01×10^{-1}
6	5.81×10^{-1}	8.35×10^{-2}	5.70×10^{-1}	8.28×10^{-2}	5.64×10^{-1}	8.87×10^{-2}

Table 5: Error of the 2D Periodic problem with exchange field and degenerated stray field under various numbers of periods $n = 1/\varepsilon$ at time $t = j\Delta t$.

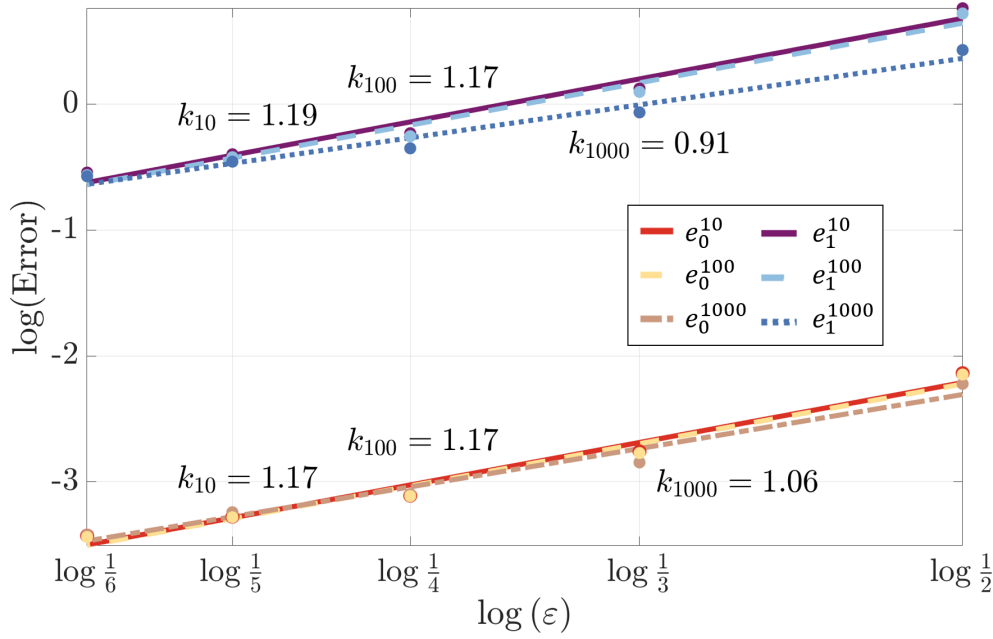


Fig. 5: Variation of error e_0^j and e_1^j relative to the cell size ε across different time steps j in the 2D Periodic problem with exchange field and degenerated stray field.

4.4. 3D Periodic problem. For the 3D case, the Periodic problem with the exchange field is considered in domain $\Omega = [0, 1]^3$. In this case, the multiscale and homogenized LLG equation are consistent with subsection 4.1. The convergence results can be expressed as

$$\begin{aligned} \|\mathbf{m}^\varepsilon(\mathbf{x}, t) - \mathbf{m}_0(\mathbf{x}, t)\|_{L^2(\Omega)} &\leq C\varepsilon^1, \\ \left\| \mathbf{m}^\varepsilon(\mathbf{x}, t) - \mathbf{m}_0(\mathbf{x}, t) - \varepsilon \chi\left(\frac{\mathbf{x}}{\varepsilon}\right) \nabla \mathbf{m}_0(\mathbf{x}, t) \right\|_{H^1(\Omega)} &\leq C\varepsilon^1. \end{aligned}$$

The spatial grid sizes of the reference and the homogenized solutions are $h = 1/30$ and $h = 1/24$, and the same time step size $\Delta t = 5 \times 10^{-5}$ is used. Moreover, the exchange coefficient is given by

$$\begin{aligned} \mathbf{a}(\mathbf{y}) &= \left(1.1 + 0.25 \cos(2\pi(y_1 - 0.5))\right) \left(1.1 + 0.25 \cos(2\pi(y_2 - 0.5))\right) \\ &\quad \cdot \left(1.1 + 0.25 \cos(2\pi(y_3 - 0.5))\right) \times I_3, \end{aligned}$$

where I_3 is the 3×3 identity matrix.

Table 6 presents the error results at different time $t = j\Delta t$ with various numbers of periods n , where the corresponding error convergence orders are depicted in Figure 6. From the figure, it can be observed that the convergence orders of the L^2 error closely align with the theoretical results. Due to limitation of the mesh size for the reference solution, the convergence orders of H^1 error exhibit a slight deviation. Specifically, the deviation at the initial time is caused by the approximation of the initial data for multiscale systems. However, the convergence orders approach the theoretical values over time.

n	$j=10$		$j=10^2$	
	e_0	\tilde{e}_0	e_0	\tilde{e}_0
2	9.51×10^{-2}	9.55×10^{-2}	9.88×10^{-2}	9.92×10^{-2}
3	6.48×10^{-2}	6.51×10^{-2}	6.52×10^{-2}	6.55×10^{-2}
5	3.72×10^{-2}	3.74×10^{-2}	3.78×10^{-2}	3.80×10^{-2}
	e_1	\tilde{e}_1	e_1	\tilde{e}_1
2	6.85×10^{-1}	1.03×10^{-1}	7.65×10^{-1}	1.13×10^{-1}
3	6.30×10^{-1}	9.47×10^{-2}	6.65×10^{-1}	9.86×10^{-2}
5	5.44×10^{-1}	8.22×10^{-2}	5.30×10^{-1}	7.93×10^{-2}

Table 6: Error of the 3D Periodic problem under various numbers of periods $n = 1/\varepsilon$ at time $t = j\Delta t$.

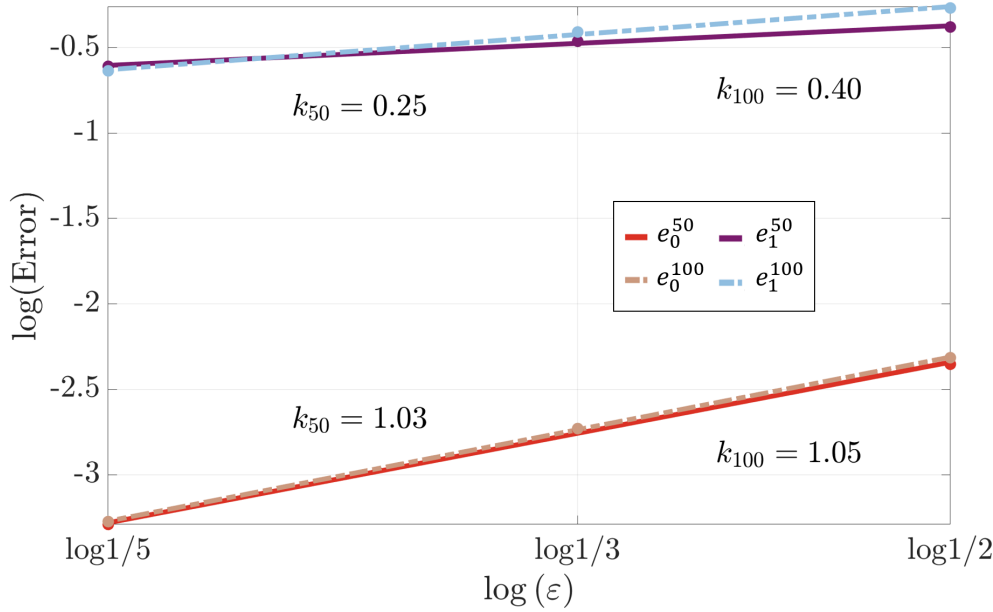


Fig. 6: Variation of error e_0^j and e_1^j relative to the cell size ε across different time steps j in the 3D Periodic problem.

5. Conclusions. In this paper, we present novel theoretical results and the corresponding numerical framework for solving the multiscale LLG equation based on the two-scale method. First, we focus on the more realistic and complex multiscale LLG model, which considers the contribution of the exchange, anisotropy, stray, and external magnetic fields. With the proper second-order corrector, we derive the approximation error of (1.2) in the H^1 norm and its uniform $W^{1,6}$ estimate. Second, a robust numerical framework is proposed, which is then employed to effectively validate the theoretical convergence order for both the Periodic and Neumann problems. Third, to overcome the computational prohibitive induced by ε , we design an improved implicit scheme for temporal discretization, which significantly reduces the required number of iterations and relaxes the constraints on the time step size. Specifically, the projection and expansion methods are proposed to overcome the inherent non-consistency in the initial data between the multiscale problem and its homogenized problem.

Moreover, magnetostriction induced by the variations in magnetization arouses the interest and finds widespread applications in practical engineering, such as magnetic displacement sensors. This physical quantity can be characterized by the system, which couples the multiscale LLG equation with the elastic wave equation [3]. In our forthcoming work, the issue will be discussed.

Appendix A. Proof of Lemma 3.6. This proof refer to the estimate of $\Theta_{\text{sf}}^\varepsilon$ in [10]. By utilizing the two-scale expansion, $\Theta_{\text{ts}}^\varepsilon$ defined in (3.9) can be rewritten in the following form

$$\begin{aligned} \Theta_{\text{ts}}^\varepsilon &= \varepsilon^{-2} \Theta_{\text{ts}}^{(-2)} \left(\mathbf{x}, \frac{\mathbf{x}}{\varepsilon} \right) + \varepsilon^{-1} \Theta_{\text{ts}}^{(-1)} \left(\mathbf{x}, \frac{\mathbf{x}}{\varepsilon} \right) \\ &\quad + \Theta_{\text{ts}}^{(0)} \left(\mathbf{x}, \frac{\mathbf{x}}{\varepsilon} \right) + \varepsilon \Theta_{\text{ts}}^{(1)} \left(\mathbf{x}, \frac{\mathbf{x}}{\varepsilon} \right) + \varepsilon^2 \Theta_{\text{ts}}^{(2)} \left(\mathbf{x}, \frac{\mathbf{x}}{\varepsilon} \right). \end{aligned}$$

For $\tilde{\mathbf{m}}^\varepsilon$ and \tilde{U}^ε defined in (2.6), it can be easily checked that $\Theta_{\text{ts}}^{(-2)} = 0$ and $\Theta_{\text{ts}}^{(-1)} = 0$. In the following, $\Theta_{\text{ts}}^{(0)} = 0$ will be proved. In fact, the zero-order term $\Theta_{\text{ts}}^{(0)}$ yields

$$\begin{aligned} \Theta_{\text{ts}}^{(0)}(\mathbf{x}, \mathbf{y}) &= \partial_t \mathbf{m}_0 - \alpha \{ \mathcal{A}_0 \mathbf{m}_2 + \mathbf{h}(\mathbf{x}, \mathbf{y}) \} \\ &\quad + \mathbf{m}_0 \times \{ \mathcal{A}_0 \mathbf{m}_2 + \mathbf{h}(\mathbf{x}, \mathbf{y}) \} - \alpha g(\mathbf{x}, \mathbf{y}) \mathbf{m}_0. \end{aligned} \tag{A.1}$$

where $\mathbf{h}(\mathbf{x}, \mathbf{y})$ and $g(\mathbf{x}, \mathbf{y})$ are defined as

$$\begin{aligned} \mathbf{h}(\mathbf{x}, \mathbf{y}) &= \mathcal{A}_1 \mathbf{m}_1 + \mathcal{A}_2 \mathbf{m}_0 + \mu \nabla_{\mathbf{x}} U_0 + \mu \nabla_{\mathbf{y}} U_1 - K (\mathbf{m}_0 \cdot \mathbf{u}) \mathbf{u} + M_s \mathbf{h}_a, \\ g(\mathbf{x}, \mathbf{y}) &= \mathbf{a} |\nabla_{\mathbf{x}} \mathbf{m}_0 + \nabla_{\mathbf{y}} \mathbf{m}_1|^2 - \mu \mathbf{m}_0 \cdot (\nabla_{\mathbf{x}} U_0 + \nabla_{\mathbf{y}} U_1) + K (\mathbf{m}_0 \cdot \mathbf{u})^2 - M_s \mathbf{m}_0 \cdot \mathbf{h}_a. \end{aligned} \tag{A.2}$$

The classical solution \mathbf{m}_0 of (2.25) satisfies

$$\partial_t \mathbf{m}_0 - \alpha \mathbf{h}_{\text{eff}}^0 + \mathbf{m}_0 \times \mathbf{h}_{\text{eff}}^0 + \alpha (\mathbf{m}_0 \cdot \mathbf{h}_{\text{eff}}^0) \mathbf{m}_0 = 0. \tag{A.3}$$

By substituting (A.3) into (A.1), we can derive that

$$\begin{aligned} \Theta_{\text{ts}}^{(0)}(\mathbf{x}, \mathbf{y}) &= -\alpha \{ \mathcal{A}_0 \mathbf{m}_2 + \mathbf{h}(\mathbf{x}, \mathbf{y}) - \mathbf{h}_{\text{eff}}^0 \} \\ &\quad + \mathbf{m}_0 \times \{ \mathcal{A}_0 \mathbf{m}_2 + \mathbf{h}(\mathbf{x}, \mathbf{y}) - \mathbf{h}_{\text{eff}}^0 \} - \alpha \{ g(\mathbf{x}, \mathbf{y}) + (\mathbf{m}_0 \cdot \mathbf{h}_{\text{eff}}^0) \} \mathbf{m}_0. \end{aligned} \tag{A.4}$$

Applying $\text{div}_{\mathbf{y}}(\mathbf{a} \nabla_{\mathbf{x}}) + \text{div}_{\mathbf{x}}(\mathbf{a} \nabla_{\mathbf{y}})$ to the both sides of geometric constraint $\mathbf{m}_0 \cdot \mathbf{m}_1 = 0$, we have

$$\begin{aligned} \text{div}_{\mathbf{y}}(\mathbf{a} \nabla_{\mathbf{x}} \mathbf{m}_0) \cdot \mathbf{m}_1 + 2 \mathbf{a} \nabla_{\mathbf{x}} \mathbf{m}_0 \cdot \nabla_{\mathbf{y}} \mathbf{m}_1 \\ + \mathbf{m}_0 \cdot \text{div}_{\mathbf{x}}(\mathbf{a} \nabla_{\mathbf{y}} \mathbf{m}_1) + \mathbf{m}_0 \cdot \text{div}_{\mathbf{y}}(\mathbf{a} \nabla_{\mathbf{x}} \mathbf{m}_1) = 0. \end{aligned}$$

Moreover, based on the definition in (2.11)-(2.12), it can be proved that

$$\mathbf{m}_1 \cdot \text{div}_{\mathbf{y}}(\mathbf{a} \nabla_{\mathbf{y}} \mathbf{m}_1) + \mathbf{m}_1 \cdot \text{div}_{\mathbf{y}}(\mathbf{a} \nabla_{\mathbf{x}} \mathbf{m}_1) = 0.$$

With the above results, it yields

$$\begin{aligned} 2 \mathbf{a} \nabla_{\mathbf{x}} \mathbf{m}_0 \cdot \nabla_{\mathbf{y}} \mathbf{m}_1 &= \mathbf{m}_1 \cdot \text{div}_{\mathbf{y}}(\mathbf{a} \nabla_{\mathbf{y}} \mathbf{m}_1) \\ &\quad - \mathbf{m}_0 \cdot \text{div}_{\mathbf{x}}(\mathbf{a} \nabla_{\mathbf{y}} \mathbf{m}_1) - \mathbf{m}_0 \cdot \text{div}_{\mathbf{y}}(\mathbf{a} \nabla_{\mathbf{x}} \mathbf{m}_1) \\ &= \mathbf{m}_1 \cdot \mathcal{A}_0 \mathbf{m}_1 - \mathbf{m}_0 \cdot \mathcal{A}_1 \mathbf{m}_1. \end{aligned}$$

Utilizing $\mathbf{a}|\nabla_{\mathbf{x}}\mathbf{m}_0|^2 = -\mathbf{m}_0 \cdot \mathcal{A}_2\mathbf{m}_0$, we have

$$(A.5) \quad \mathbf{a}|\nabla_{\mathbf{x}}\mathbf{m}_0 + \nabla_{\mathbf{y}}\mathbf{m}_1|^2 = -\mathbf{m}_0 \cdot (\mathcal{A}_2\mathbf{m}_0 + \mathcal{A}_1\mathbf{m}_1) + \mathbf{m}_1 \cdot \mathcal{A}_0\mathbf{m}_1 + \mathbf{a}|\nabla_{\mathbf{y}}\mathbf{m}_1|^2.$$

Combining (A.5) with (A.2), it can be derived that

$$(A.6) \quad \begin{aligned} g(\mathbf{x}, \mathbf{y}) &= -\mathbf{m}_0 \cdot (\mathcal{A}_2\mathbf{m}_0 + \mathcal{A}_1\mathbf{m}_1) + \mathbf{m}_1 \cdot \mathcal{A}_0\mathbf{m}_1 + \mathbf{a}|\nabla_{\mathbf{y}}\mathbf{m}_1|^2 \\ &\quad + \mu\mathbf{m}_0 \cdot (\nabla_{\mathbf{x}}U_0 + \nabla_{\mathbf{y}}U_1) - K(\mathbf{m}_0 \cdot \mathbf{u})^2 + M_s\mathbf{m}_0 \cdot \mathbf{h}_a \\ &= -\mathbf{m}_0 \cdot \mathbf{h}(\mathbf{x}, \mathbf{y}) + \mathbf{m}_1 \cdot \mathcal{A}_0\mathbf{m}_1 + \mathbf{a}|\nabla_{\mathbf{y}}\mathbf{m}_1|^2. \end{aligned}$$

Substituting (A.6) into (A.4), we have

$$(A.7) \quad \begin{aligned} \Theta_{\text{ts}}^{(0)}(\mathbf{x}, \mathbf{y}) &= -\alpha \{ \mathcal{A}_0\mathbf{m}_2 + \mathbf{h}(\mathbf{x}, \mathbf{y}) - \mathbf{h}_{\text{eff}}^0 \} + \mathbf{m}_0 \times \{ \mathcal{A}_0\mathbf{m}_2 + \mathbf{h}(\mathbf{x}, \mathbf{y}) - \mathbf{h}_{\text{eff}}^0 \} \\ &\quad + \alpha\mathbf{m}_0 \cdot \{ \mathbf{h}(\mathbf{x}, \mathbf{y}) - \mathbf{h}_{\text{eff}}^0 \} \mathbf{m}_0 - \alpha(\mathbf{m}_1 \cdot \mathcal{A}_0\mathbf{m}_1 + \mathbf{a}|\nabla_{\mathbf{y}}\mathbf{m}_1|^2)\mathbf{m}_0. \end{aligned}$$

Combing (2.20) with (A.7), it can derive that $\Theta_{\text{ts}}^{(0)} = 0$. With the above results, we have

$$(A.8) \quad \Theta_{\text{ts}}^\varepsilon \left(\mathbf{x}, \frac{\mathbf{x}}{\varepsilon} \right) = \varepsilon \Theta_{\text{ts}}^{(1)} \left(\mathbf{x}, \frac{\mathbf{x}}{\varepsilon} \right) + \varepsilon^2 \Theta_{\text{ts}}^{(2)} \left(\mathbf{x}, \frac{\mathbf{x}}{\varepsilon} \right).$$

Furthermore, it can be checked that the remainder terms $\Theta_{\text{ts}}^{(1)}$ and $\Theta_{\text{ts}}^{(2)}$ satisfy

$$(A.9) \quad \left\| \Theta_{\text{ts}}^{(1)} \left(\mathbf{x}, \frac{\mathbf{x}}{\varepsilon} \right) \right\|_{L^2(\Omega)} + \left\| \Theta_{\text{ts}}^{(2)} \left(\mathbf{x}, \frac{\mathbf{x}}{\varepsilon} \right) \right\|_{L^2(\Omega)} \leq C,$$

where the constant C depends on $\|\mathbf{m}_0\|_{W^{4,\infty}(\Omega)}$ and C_{coe} . Then, Lemma 3.6 can be derived by (A.8) and (A.9). The proof is completed.

Appendix B. Proof of Lemma 3.7. The following proposition about the stray field has been proved in [24].

PROPOSITION B.1. *Let $\dot{W}^{1,p}$ denote the Beppo-levi space ($1 < p < +\infty$). For any vector function $\mathbf{f} \in [L^p(\mathbb{R}^3)]^3$, there exists unique solution $U \in \dot{W}^{1,p}(\mathbb{R}^3)$ such that*

$$\Delta U = \text{div } \mathbf{f}, \quad \text{in } D'(\mathbb{R}^3),$$

and the solution satisfies the estimate

$$\|\nabla U\|_{L^p(\mathbb{R}^3)} \leq C\|\mathbf{f}\|_{L^p(\mathbb{R}^3)}.$$

Based on Proposition B.1, for $1 < p < +\infty$, one can derive that

$$(B.1) \quad \begin{aligned} \|\nabla \Psi^\varepsilon\|_{L^p(\Omega)} &\leq C_p \|\mathbf{e}^\varepsilon\|_{L^p(\Omega)}, \quad \|\nabla U^\varepsilon\|_{L^p(\Omega)} \leq C_p \|\mathbf{m}^\varepsilon\|_{L^p(\Omega)}, \\ \|\nabla \Gamma^\varepsilon\|_{L^p(\Omega)} &\leq C_p \|\tilde{\mathbf{m}}^\varepsilon\|_{L^p(\Omega)}. \end{aligned}$$

By the $W^{1,p}$ estimate of the oscillatory elliptic problem, the following inequalities are also introduced.

PROPOSITION B.2. *Given $u \in H^2(\Omega)$, then it holds that*

$$\|\nabla u\|_{L^6(\Omega)} \leq C\|\mathcal{A}_\varepsilon u\|_{L^2(\Omega)} + C\|\nabla u\|_{L^2(\Omega)},$$

where the constant C is independent of ε .

Proof. Denote $\boldsymbol{\nu} \cdot \mathbf{a}^\varepsilon \nabla u = g$ on $\partial\Omega$ and refer to Theorem 6.3.2 in [27], we have

$$\|\nabla u\|_{L^6(\Omega)} \leq C\|\mathcal{A}_\varepsilon u\|_{L^2(\Omega)} + C\|g\|_{B^{-1/2,2}(\partial\Omega)}.$$

Moreover, one can apply the following trace theorem

$$\|g\|_{B^{-1/2,2}(\partial\Omega)} \leq C\|\nabla u\|_{L^2(\Omega)} + C\|\mathcal{A}_\varepsilon u\|_{L^2(\Omega)}.$$

Then the Proposition can be proved. \square

With the above results, Lemma 3.7 can be proved as follows.

Step 1: $L^2(\Omega)$ estimate. Taking the $L^2(\Omega)$ inner product of (3.11) and \mathbf{e}^ε , it can be derived that

$$(B.2) \quad \begin{aligned} & \frac{1}{2} \frac{d}{dt} \int_{\Omega} |\mathbf{e}^\varepsilon|^2 d\mathbf{x} - \alpha \int_{\Omega} \tilde{\mathcal{H}}_e^\varepsilon(\mathbf{e}^\varepsilon, \Psi^\varepsilon) \cdot \mathbf{e}^\varepsilon d\mathbf{x} \\ &= - \int_{\Omega} \mathbf{D}_1(\mathbf{e}^\varepsilon, \Psi^\varepsilon) \cdot \mathbf{e}^\varepsilon d\mathbf{x} - \int_{\Omega} \mathbf{D}_2(\mathbf{e}^\varepsilon, \Psi^\varepsilon) \cdot \mathbf{e}^\varepsilon d\mathbf{x} + \int_{\Omega} \mathbf{F} \cdot \mathbf{e}^\varepsilon d\mathbf{x}, \end{aligned}$$

where $\mathbf{F} = -(\boldsymbol{\Theta}_{ts}^\varepsilon + \boldsymbol{\Theta}_{sf}^\varepsilon)$. Using estimate (B.1) and integration by parts for the second term on the left-hand side of (B.2), it follows that

$$(B.3) \quad - \int_{\Omega} \tilde{\mathcal{H}}_e^\varepsilon(\mathbf{e}^\varepsilon, \Psi^\varepsilon) \cdot \mathbf{e}^\varepsilon d\mathbf{x} \geq \sum_{i,j=1}^n \int_{\Omega} a_{ij}^\varepsilon \frac{\partial \mathbf{e}^\varepsilon}{\partial x_i} \cdot \frac{\partial \mathbf{e}^\varepsilon}{\partial x_j} d\mathbf{x} - C \int_{\Omega} |\mathbf{e}^\varepsilon|^2 d\mathbf{x}.$$

Based on the same idea of (B.2) and (B.3) with Young's inequality, the first term on the right-hand side of (B.2) can be estimated by

$$- \int_{\Omega} \mathbf{D}_1(\mathbf{e}^\varepsilon, \Psi^\varepsilon) \cdot \mathbf{e}^\varepsilon d\mathbf{x} \leq C \int_{\Omega} |\mathbf{e}^\varepsilon|^2 d\mathbf{x} + \delta C \int_{\Omega} |\nabla \mathbf{e}^\varepsilon|^2 d\mathbf{x}.$$

For the second term on the right-hand side of (B.2), the following estimates are used

$$\left\{ \begin{aligned} & \int_{\Omega} (\nabla \mathbf{e}^\varepsilon \cdot \mathbf{a}^\varepsilon \nabla \mathbf{m}^\varepsilon) \mathbf{m}^\varepsilon \cdot \mathbf{e}^\varepsilon d\mathbf{x} \leq C \|\nabla \mathbf{m}^\varepsilon\|_{L^6(\Omega)} \|\mathbf{e}^\varepsilon\|_{L^3(\Omega)} \|\nabla \mathbf{e}^\varepsilon\|_{L^2(\Omega)}, \\ & \int_{\Omega} (\mu^\varepsilon \mathbf{e}^\varepsilon \cdot \nabla U^\varepsilon) \mathbf{m}^\varepsilon \cdot \mathbf{e}^\varepsilon d\mathbf{x} \leq C \|\nabla U^\varepsilon\|_{L^6(\Omega)} \|\mathbf{e}^\varepsilon\|_{L^3(\Omega)} \|\mathbf{e}^\varepsilon\|_{L^2(\Omega)}, \\ & \int_{\Omega} (\mu^\varepsilon \tilde{\mathbf{m}}^\varepsilon \cdot \nabla \Psi^\varepsilon) \mathbf{m}^\varepsilon \cdot \mathbf{e}^\varepsilon d\mathbf{x} \leq C \|\nabla \Psi^\varepsilon\|_{L^6(\Omega)} \|\mathbf{e}^\varepsilon\|_{L^3(\Omega)} \|\mathbf{e}^\varepsilon\|_{L^2(\Omega)}, \end{aligned} \right.$$

Moreover, applying (B.1) and Young's inequality, together with the embedding theorem of the $H^1(\Omega)$ space into $L^p(\Omega)$ space for $1 \leq p \leq 6$, we have

$$- \int_{\Omega} \mathbf{D}_2(\mathbf{e}^\varepsilon, \Psi^\varepsilon) \cdot \mathbf{e}^\varepsilon d\mathbf{x} \leq C \|\mathbf{e}^\varepsilon\|_{L^2(\Omega)}^2 + \delta C \|\mathbf{e}^\varepsilon\|_{H^1(\Omega)}^2,$$

where C depends on $\|\nabla \mathbf{m}^\varepsilon\|_{L^6(\Omega)}$, $\|\nabla \tilde{\mathbf{m}}^\varepsilon\|_{L^6(\Omega)}$, $\|\nabla U^\varepsilon\|_{L^6(\Omega)}$, $\|\nabla \Gamma^\varepsilon\|_{L^6(\Omega)}$, $\|\mathbf{m}^\varepsilon\|_{L^\infty(\Omega)}$ and $\|\tilde{\mathbf{m}}^\varepsilon\|_{L^\infty(\Omega)}$. For the last term in (B.2), the following estimate can be deduced by Young's inequality and Sobolev inequality

$$\int_{\Omega} \mathbf{F} \cdot \mathbf{e}^\varepsilon d\mathbf{x} \leq C \|\boldsymbol{\Theta}_{ts}^\varepsilon\|_{L^2(\Omega)}^2 + C \|\mathbf{e}^\varepsilon\|_{L^2(\Omega)} + C \|\boldsymbol{\Theta}_{sf}^\varepsilon\|_{L^{6/5}(\Omega)}^2 + \delta C \|\mathbf{e}^\varepsilon\|_{H^1(\Omega)},$$

with any small $\delta > 0$. Utilizing the above estimates, it can be obtained from (B.2) that

$$(B.4) \quad \begin{aligned} & \frac{1}{2} \frac{d}{dt} \|\mathbf{e}^\varepsilon\|_{L^2(\Omega)}^2 + (\alpha a_{\min} - C\delta) \|\nabla \mathbf{e}^\varepsilon\|_{L^2(\Omega)}^2 \\ & \leq C \|\mathbf{e}^\varepsilon\|_{L^2(\Omega)}^2 + C \|\Theta_{\text{ts}}^\varepsilon\|_{L^2(\Omega)}^2 + C \|\Theta_{\text{sf}}^\varepsilon\|_{L^{6/5}(\Omega)}^2. \end{aligned}$$

Let $\delta \rightarrow 0$, the estimate (3.13) in Lemma 3.7 can be directly deduced by Grönwall's inequality.

Step 2: $H^1(\Omega)$ estimate. Taking the $L^2(\Omega)$ inner product of (3.11) and $\tilde{\mathcal{H}}_e^\varepsilon(\mathbf{e}^\varepsilon, \Psi^\varepsilon)$, we obtain

$$(B.5) \quad \begin{aligned} & - \int_{\Omega} \partial_t \mathbf{e}^\varepsilon \cdot \tilde{\mathcal{H}}_e^\varepsilon(\mathbf{e}^\varepsilon, \Psi^\varepsilon) d\mathbf{x} + \alpha \int_{\Omega} \tilde{\mathcal{H}}_e^\varepsilon(\mathbf{e}^\varepsilon, \Psi^\varepsilon) \cdot \tilde{\mathcal{H}}_e^\varepsilon(\mathbf{e}^\varepsilon, \Psi^\varepsilon) d\mathbf{x} \\ & = \int_{\Omega} \mathbf{D}_1(\mathbf{e}^\varepsilon, \Psi^\varepsilon) \cdot \tilde{\mathcal{H}}_e^\varepsilon(\mathbf{e}^\varepsilon, \Psi^\varepsilon) d\mathbf{x} + \int_{\Omega} \mathbf{D}_2(\mathbf{e}^\varepsilon, \Psi^\varepsilon) \cdot \tilde{\mathcal{H}}_e^\varepsilon(\mathbf{e}^\varepsilon, \Psi^\varepsilon) d\mathbf{x} \\ & \quad - \int_{\Omega} \mathbf{F} \cdot \tilde{\mathcal{H}}_e^\varepsilon(\mathbf{e}^\varepsilon, \Psi^\varepsilon) d\mathbf{x}. \end{aligned}$$

Subsequently, the term-by-term estimates for (B.5) are provided. The integration by parts on the first term of (B.5) yields

$$- \int_{\Omega} \partial_t \mathbf{e}^\varepsilon \cdot \tilde{\mathcal{H}}_e^\varepsilon(\mathbf{e}^\varepsilon, \Psi^\varepsilon) d\mathbf{x} = \frac{d}{dt} \mathcal{G}_{\mathcal{L}}^\varepsilon[\mathbf{e}^\varepsilon, \Psi^\varepsilon].$$

Here, $\mathcal{G}_{\mathcal{L}}^\varepsilon[\mathbf{e}^\varepsilon, \Psi^\varepsilon] = \int_{\Omega} g_{\mathcal{L}}^\varepsilon(\mathbf{e}^\varepsilon, \Psi^\varepsilon) d\mathbf{x}$ is the total energy, with the energy density $g_{\mathcal{L}}^\varepsilon$ defined in (3.6). Using $\mathbf{m}^\varepsilon \times \tilde{\mathcal{H}}_e^\varepsilon(\mathbf{e}^\varepsilon, \Psi^\varepsilon) \cdot \tilde{\mathcal{H}}_e^\varepsilon(\mathbf{e}^\varepsilon, \Psi^\varepsilon) = 0$, the first term on the right-hand side of (B.5) can be estimated by Sobolev inequality

$$\begin{aligned} \int_{\Omega} \mathbf{D}_1(\mathbf{e}^\varepsilon, \Psi^\varepsilon) \cdot \tilde{\mathcal{H}}_e^\varepsilon(\mathbf{e}^\varepsilon, \Psi^\varepsilon) d\mathbf{x} & \leq C \|\mathcal{H}_e^\varepsilon(\tilde{\mathbf{m}}^\varepsilon, \Gamma^\varepsilon)\|_{L^3(\Omega)} \|\mathbf{e}^\varepsilon\|_{L^6(\Omega)} \|\tilde{\mathcal{H}}_e^\varepsilon(\mathbf{e}^\varepsilon, \Psi^\varepsilon)\|_{L^2(\Omega)} \\ & \leq C \|\mathbf{e}^\varepsilon\|_{H^1(\Omega)}^2 + \delta C \|\tilde{\mathcal{H}}_e^\varepsilon(\mathbf{e}^\varepsilon, \Psi^\varepsilon)\|_{L^2(\Omega)}^2, \end{aligned}$$

where $C = C^0(1 + \|\mathcal{H}_e^\varepsilon(\tilde{\mathbf{m}}^\varepsilon, \Gamma^\varepsilon)\|_{L^3(\Omega)}^2)$. For the second term on the right-hand side of (B.5), the following estimates are used

$$\left\{ \begin{aligned} & \int_{\Omega} (\nabla \mathbf{e}^\varepsilon \cdot \mathbf{a}^\varepsilon \nabla \mathbf{m}^\varepsilon) \mathbf{m}^\varepsilon \cdot \tilde{\mathcal{H}}_e^\varepsilon(\mathbf{e}^\varepsilon, \Psi^\varepsilon) d\mathbf{x} \leq C \|\nabla \mathbf{m}^\varepsilon\|_{L^6(\Omega)} \|\nabla \mathbf{e}^\varepsilon\|_{L^3(\Omega)} \|\tilde{\mathcal{H}}_e^\varepsilon(\mathbf{e}^\varepsilon, \Psi^\varepsilon)\|_{L^2(\Omega)}, \\ & \int_{\Omega} (\mu^\varepsilon \mathbf{e}^\varepsilon \cdot \nabla U^\varepsilon) \mathbf{m}^\varepsilon \cdot \tilde{\mathcal{H}}_e^\varepsilon(\mathbf{e}^\varepsilon, \Psi^\varepsilon) d\mathbf{x} \leq C \|\nabla U^\varepsilon\|_{L^6(\Omega)} \|\mathbf{e}^\varepsilon\|_{L^3(\Omega)} \|\tilde{\mathcal{H}}_e^\varepsilon(\mathbf{e}^\varepsilon, \Psi^\varepsilon)\|_{L^2(\Omega)}, \\ & \int_{\Omega} (\mu^\varepsilon \tilde{\mathbf{m}}^\varepsilon \cdot \nabla \Psi^\varepsilon) \mathbf{m}^\varepsilon \cdot \tilde{\mathcal{H}}_e^\varepsilon(\mathbf{e}^\varepsilon, \Psi^\varepsilon) d\mathbf{x} \leq C \|\tilde{\mathbf{m}}^\varepsilon\|_{L^\infty(\Omega)} \|\nabla \Psi^\varepsilon\|_{L^2(\Omega)} \|\tilde{\mathcal{H}}_e^\varepsilon(\mathbf{e}^\varepsilon, \Psi^\varepsilon)\|_{L^2(\Omega)}. \end{aligned} \right.$$

Moreover, employing interpolation inequality and Proposition B.2, it can be derived

$$\begin{aligned} \|\nabla \mathbf{e}^\varepsilon\|_{L^3(\Omega)} & \leq \|\nabla \mathbf{e}^\varepsilon\|_{L^2(\Omega)}^{1/2} \|\nabla \mathbf{e}^\varepsilon\|_{L^6(\Omega)}^{1/2} \\ & \leq C \|\nabla \mathbf{e}^\varepsilon\|_{L^2(\Omega)}^{1/2} (\|\mathcal{A}_\varepsilon \mathbf{e}^\varepsilon\|_{L^2(\Omega)} + \|\nabla \mathbf{e}^\varepsilon\|_{L^2(\Omega)})^{1/2} \\ & \leq C \|\nabla \mathbf{e}^\varepsilon\|_{L^2(\Omega)}^{1/2} (1 + \|\tilde{\mathcal{H}}_e^\varepsilon(\mathbf{e}^\varepsilon, \Psi^\varepsilon)\|_{L^2(\Omega)} + \|\nabla \mathbf{e}^\varepsilon\|_{L^2(\Omega)})^{1/2}. \end{aligned}$$

Combining the above estimates with (B.1), it yields

$$\int_{\Omega} \mathbf{D}_2(\mathbf{e}^\varepsilon, \Psi^\varepsilon) \cdot \tilde{\mathcal{H}}_e^\varepsilon(\mathbf{e}^\varepsilon, \Psi^\varepsilon) d\mathbf{x} \leq C + C \|\mathbf{e}^\varepsilon\|_{H^1(\Omega)}^2 + \delta \|\tilde{\mathcal{H}}_e^\varepsilon(\mathbf{e}^\varepsilon, \Psi^\varepsilon)\|_{L^2(\Omega)}^2,$$

where the constant C depends on $\|\mathbf{m}^\varepsilon\|_{W^{1,\infty}(\Omega)}$, $\|\tilde{\mathbf{m}}^\varepsilon\|_{W^{1,\infty}(\Omega)}$, $\|\nabla U^\varepsilon\|_{L^6(\Omega)}$, and $\|\nabla \Gamma^\varepsilon\|_{L^6(\Omega)}$. For the last term in (B.5), we have

$$\int_{\Omega} \mathbf{F} \cdot \tilde{\mathcal{H}}_e^\varepsilon(\mathbf{e}^\varepsilon, \Psi^\varepsilon) \, d\mathbf{x} \leq C \|\mathbf{F}\|_{L^2(\Omega)}^2 + \delta \|\tilde{\mathcal{H}}_e^\varepsilon(\mathbf{e}^\varepsilon, \Psi^\varepsilon)\|_{L^2(\Omega)}^2.$$

Substituting the above results into (B.5), it can be derived that

$$\frac{d}{dt} \mathcal{G}_L^\varepsilon[\mathbf{e}^\varepsilon, \Psi^\varepsilon] + (\alpha - C\delta) \|\tilde{\mathcal{H}}_e^\varepsilon(\mathbf{e}^\varepsilon, \Psi^\varepsilon)\|_{L^2(\Omega)}^2 \leq C (\|\mathbf{e}^\varepsilon\|_{H^1(\Omega)}^2 + \|\mathbf{F}\|_{L^2(\Omega)}^2).$$

Integrating the above inequality over $[0, t]$ for $0 < t < T$ and using the following equation

$$\mathcal{G}_L^\varepsilon[\mathbf{e}^\varepsilon, \Psi^\varepsilon] \geq \frac{a_{\min}}{2} \|\nabla \mathbf{e}^\varepsilon\|_{L^2(\Omega)}^2 - C,$$

one can finally derive

$$\begin{aligned} \frac{a_{\min}}{2} \|\nabla \mathbf{e}^\varepsilon(t)\|_{L^2(\Omega)}^2 + (\alpha - C\delta) \int_0^t \|\tilde{\mathcal{H}}_e^\varepsilon(\mathbf{e}^\varepsilon, \Psi^\varepsilon)\|_{L^2(\Omega)}^2 \, d\tau \\ \leq C \int_0^t (\|\mathbf{e}^\varepsilon\|_{L^2(\Omega)}^2 + \|\nabla \mathbf{e}^\varepsilon\|_{L^2(\Omega)}^2 + \|\mathbf{F}\|_{L^2(\Omega)}^2) \, d\tau. \end{aligned}$$

Let $\delta \rightarrow 0$, the estimate (3.14) in Lemma 3.7 can be directly deduced by Grönwall's inequality. The proof is completed.

Appendix C. Proof of Lemma 3.8. The following estimates will be used:

$$(C.1) \quad a_{\max}^{-1} \|\mathbf{m}^\varepsilon \cdot \mathcal{A}_\varepsilon \mathbf{m}^\varepsilon\|_{L^3(\Omega)}^3 \leq \|\nabla \mathbf{m}^\varepsilon\|_{L^6(\Omega)}^6 \leq a_{\min}^{-1} \|\mathcal{A}_\varepsilon \mathbf{m}^\varepsilon\|_{L^3(\Omega)}^3,$$

$$(C.2) \quad \|\mathcal{A}_\varepsilon \mathbf{m}^\varepsilon\|_{L^p(\Omega)} - C_p \leq \|\mathcal{H}_e^\varepsilon(\mathbf{m}^\varepsilon, U^\varepsilon)\|_{L^p(\Omega)} \leq \|\mathcal{A}_\varepsilon \mathbf{m}^\varepsilon\|_{L^p(\Omega)} + C_p,$$

with $1 < p < +\infty$. Here, (C.1) can be derived by $-\mathbf{a}^\varepsilon |\nabla \mathbf{m}^\varepsilon|^2 = \mathbf{m}^\varepsilon \cdot \mathcal{A}_\varepsilon \mathbf{m}^\varepsilon$ with $|\mathbf{m}^\varepsilon| = 1$ and the symmetry of \mathbf{a}^ε in Assumption (I). (C.2) can be derived by the estimate (B.1). For any vector \mathbf{v} , an orthogonal decomposition is given by

$$(C.3) \quad \mathbf{v} = (\mathbf{m}^\varepsilon \cdot \mathbf{v}) \mathbf{m}^\varepsilon - \mathbf{m}^\varepsilon \times (\mathbf{m}^\varepsilon \times \mathbf{v}).$$

In the following, we introduce an interpolation inequality of the effective field $\mathcal{H}_e^\varepsilon$ defined in (3.5).

LEMMA C.1. *Given $\mathbf{m}^\varepsilon \in H^3(\Omega)$, U^ε that satisfies (3.7), $|\mathbf{m}^\varepsilon| = 1$ and the Neumann boundary condition $\boldsymbol{\nu} \cdot \mathbf{a}^\varepsilon \nabla \mathbf{m}^\varepsilon = 0$. Then it holds for any $0 < \delta < 1$*

$$(C.4) \quad \|\mathcal{H}_e^\varepsilon(\mathbf{m}^\varepsilon, U^\varepsilon)\|_{L^3(\Omega)}^3 \leq C_\delta + C_\delta \|\mathcal{H}_e^\varepsilon(\mathbf{m}^\varepsilon, U^\varepsilon)\|_{L^2(\Omega)}^6 + \delta \|\mathbf{m}^\varepsilon \times \nabla \mathcal{H}_e^\varepsilon(\mathbf{m}^\varepsilon, U^\varepsilon)\|_{L^2(\Omega)}^2,$$

where the constant C_δ depends on δ , but is independent of ε .

Proof. Applying decomposition (C.3) with $\mathbf{v} = \mathcal{H}_e^\varepsilon(\mathbf{m}^\varepsilon, U^\varepsilon)$, we have

$$(C.5) \quad \begin{aligned} \|\mathcal{H}_e^\varepsilon(\mathbf{m}^\varepsilon, U^\varepsilon)\|_{L^3(\Omega)}^3 &\leq \int_{\Omega} |\mathbf{m}^\varepsilon \cdot \mathcal{H}_e^\varepsilon(\mathbf{m}^\varepsilon, U^\varepsilon)|^3 \, d\mathbf{x} \\ &+ \int_{\Omega} |\mathbf{m}^\varepsilon \times \mathcal{H}_e^\varepsilon(\mathbf{m}^\varepsilon, U^\varepsilon)|^3 \, d\mathbf{x} =: \mathcal{I}_1 + \mathcal{I}_2. \end{aligned}$$

Then, the right-hand side of (C.5) is estimated as follows. For \mathcal{I}_1 , it can be derived by applying (C.1)-(C.2) and Proposition B.2

$$(C.6) \quad \mathcal{I}_1 \leq C + C \|\nabla \mathbf{m}^\varepsilon\|_{L^6(\Omega)}^6 \leq C + C \|\mathcal{H}_e^\varepsilon(\mathbf{m}^\varepsilon, U^\varepsilon)\|_{L^2(\Omega)}^6.$$

As for \mathcal{I}_2 , with Sobolev inequality for $n \leq 3$, we have

$$(C.7) \quad \mathcal{I}_2 \leq C + C \|\mathbf{m}^\varepsilon \times \mathcal{H}_e^\varepsilon(\mathbf{m}^\varepsilon, U^\varepsilon)\|_{L^2(\Omega)}^6 + \delta^* \|\mathbf{m}^\varepsilon \times \mathcal{H}_e^\varepsilon(\mathbf{m}^\varepsilon, U^\varepsilon)\|_{H^1(\Omega)}^2.$$

For the last term of (C.7), by applying (C.1)-(C.2), it can be proved that

$$\begin{aligned} \delta^* \|\nabla \mathbf{m}^\varepsilon \times \mathcal{H}_e^\varepsilon(\mathbf{m}^\varepsilon)\|_{L^2(\Omega)}^2 &\leq \delta^* \|\nabla \mathbf{m}^\varepsilon\|_{L^6(\Omega)}^6 + \delta^* \|\mathcal{H}_e^\varepsilon(\mathbf{m}^\varepsilon, U^\varepsilon)\|_{L^3(\Omega)}^3 \\ &\leq C + C \delta^* \|\mathcal{H}_e^\varepsilon(\mathbf{m}^\varepsilon, U^\varepsilon)\|_{L^3(\Omega)}^3. \end{aligned}$$

Combining (C.6), (C.7) with (C.5), one can finally derive

$$\begin{aligned} (1 - C\delta^*) \|\mathcal{H}_e^\varepsilon(\mathbf{m}^\varepsilon, U^\varepsilon)\|_{L^3(\Omega)}^3 &\leq C + C \|\mathcal{H}_e^\varepsilon(\mathbf{m}^\varepsilon, U^\varepsilon)\|_{L^2(\Omega)}^6 \\ &\quad + \delta^* \|\mathbf{m}^\varepsilon \times \nabla \mathcal{H}_e^\varepsilon(\mathbf{m}^\varepsilon, U^\varepsilon)\|_{L^2(\Omega)}^2. \end{aligned}$$

Let $\delta^* < \frac{1}{2C}$, (C.4) can be derived by $\delta = \delta^*/(1 - C\delta^*) < 1$. \square

In the following, we present the results about uniform boundedness. The multi-scale LLG equation (3.7) can be rewritten into a degenerate form by using the vector triple product formula (2.33)

$$(C.8) \quad \partial_t \mathbf{m}^\varepsilon + \alpha \mathbf{m}^\varepsilon \times (\mathbf{m}^\varepsilon \times \mathcal{H}_e^\varepsilon(\mathbf{m}^\varepsilon, U^\varepsilon)) + \mathbf{m}^\varepsilon \times \mathcal{H}_e^\varepsilon(\mathbf{m}^\varepsilon, U^\varepsilon) = 0.$$

Multiplying (C.8) by $\mathcal{H}_e^\varepsilon(\mathbf{m}^\varepsilon, U^\varepsilon)$ and integrating over $(0, t)$, the energy dissipation identity can be given by

$$(C.9) \quad \mathcal{G}_L^\varepsilon[\mathbf{m}^\varepsilon(t), U^\varepsilon(t)] + \alpha \int_0^t \|\mathbf{m}^\varepsilon \times \mathcal{H}_e^\varepsilon(\mathbf{m}^\varepsilon)\|_{L^2(\Omega)}^2 d\tau = \mathcal{G}_L^\varepsilon[\mathbf{m}^\varepsilon(0), U^\varepsilon(0)],$$

The integrability of kinetic energy $\|\partial_t \mathbf{m}^\varepsilon\|_{L^2(\Omega)}^2$ can be induced by (C.8) and (C.9)

$$(C.10) \quad \int_0^t \|\partial_t \mathbf{m}^\varepsilon\|_{L^2(\Omega)}^2 d\tau \leq C.$$

The energy identity (C.9) implies the uniform boundedness of $\|\mathbf{m}^\varepsilon \times \mathcal{A}_\varepsilon \mathbf{m}^\varepsilon\|_{L^2(\Omega)}^2$. However, due to the degeneracy caused by the outer product, it is not enough to prove the boundedness of $\|\mathcal{A}_\varepsilon \mathbf{m}^\varepsilon\|_{L^2(\Omega)}^2$. To handle this problem, the following lemma is introduced.

LEMMA C.2. *Let $\mathbf{m}^\varepsilon \in L^2([0, T]; H^3(\Omega))$ be a solution to (2.24), then there exists $T^* \in (0, T]$ independent of ε , such that for $0 \leq t \leq T^*$,*

$$\|\mathcal{A}_\varepsilon \mathbf{m}^\varepsilon(t)\|_{L^2(\Omega)}^2 + \int_0^t \|\mathbf{m}^\varepsilon \times \nabla \mathcal{H}_e^\varepsilon(\mathbf{m}^\varepsilon, U^\varepsilon)(\tau)\|_{L^2(\Omega)}^2 d\tau \leq C.$$

Therefore, by Proposition B.2, it holds

$$\|\nabla \mathbf{m}^\varepsilon(\cdot, t)\|_{L^6(\Omega)}^2 \leq C,$$

where C is a constant independent of ε and t .

Proof. Applying ∇ to (C.8) and multiplying it by $\mathbf{a}^\varepsilon \nabla \mathcal{H}_e^\varepsilon(\mathbf{m}^\varepsilon, U^\varepsilon)$, it leads to

$$\begin{aligned}
& - \int_{\Omega} \nabla(\partial_t \mathbf{m}^\varepsilon) \cdot \mathbf{a}^\varepsilon \nabla \mathcal{H}_e^\varepsilon(\mathbf{m}^\varepsilon, U^\varepsilon) \, d\mathbf{x} \\
\text{(C.11)} \quad & = \alpha \int_{\Omega} \nabla \left(\mathbf{m}^\varepsilon \times (\mathbf{m}^\varepsilon \times \mathcal{H}_e^\varepsilon(\mathbf{m}^\varepsilon, U^\varepsilon)) \right) \cdot \mathbf{a}^\varepsilon \nabla \mathcal{H}_e^\varepsilon(\mathbf{m}^\varepsilon, U^\varepsilon) \, d\mathbf{x} \\
& + \sum_{i,j=1}^n \int_{\Omega} \frac{\partial}{\partial x_i} \mathbf{m}^\varepsilon \times \mathcal{H}_e^\varepsilon(\mathbf{m}^\varepsilon, U^\varepsilon) \cdot a_{ij}^\varepsilon \frac{\partial}{\partial x_j} \mathcal{H}_e^\varepsilon(\mathbf{m}^\varepsilon, U^\varepsilon) \, d\mathbf{x} =: \mathcal{J}_1 + \mathcal{J}_2.
\end{aligned}$$

Denote $\Gamma^\varepsilon(\mathbf{m}^\varepsilon, U^\varepsilon) = \mathcal{H}_e^\varepsilon(\mathbf{m}^\varepsilon, U^\varepsilon) - \mathcal{A}_\varepsilon \mathbf{m}^\varepsilon$. With integration by parts, the left-hand side of (C.11) becomes

$$- \int_{\Omega} \nabla(\partial_t \mathbf{m}^\varepsilon) \cdot \mathbf{a}^\varepsilon \nabla \mathcal{H}_e^\varepsilon(\mathbf{m}^\varepsilon, U^\varepsilon) \, d\mathbf{x} = \int_{\Omega} \mathcal{A}_\varepsilon(\partial_t \mathbf{m}^\varepsilon) \cdot (\mathcal{A}_\varepsilon \mathbf{m}^\varepsilon + \Gamma^\varepsilon(\mathbf{m}^\varepsilon, U^\varepsilon)) \, d\mathbf{x},$$

where the right-hand side can be rewritten as

$$\frac{1}{2} \frac{d}{dt} \int_{\Omega} |\mathcal{A}_\varepsilon \mathbf{m}^\varepsilon|^2 \, d\mathbf{x} + \frac{d}{dt} \int_{\Omega} \mathcal{A}_\varepsilon \mathbf{m}^\varepsilon \cdot \Gamma^\varepsilon(\mathbf{m}^\varepsilon, U^\varepsilon) \, d\mathbf{x} - \int_{\Omega} \mathcal{A}_\varepsilon \mathbf{m}^\varepsilon \cdot \Gamma^\varepsilon(\partial_t \mathbf{m}^\varepsilon, \partial_t U^\varepsilon) \, d\mathbf{x}.$$

Then, the right-hand side of (C.11) are considered. For \mathcal{J}_1 , it can be derived by swapping the order of mixed product

$$\mathcal{J}_1 = -\alpha \sum_{i,j=1}^n \int_{\Omega} \left(\mathbf{m}^\varepsilon \times \frac{\partial}{\partial x_i} \mathcal{H}_e^\varepsilon(\mathbf{m}^\varepsilon, U^\varepsilon) \right) \cdot a_{ij}^\varepsilon \left(\mathbf{m}^\varepsilon \times \frac{\partial}{\partial x_j} \mathcal{H}_e^\varepsilon(\mathbf{m}^\varepsilon, U^\varepsilon) \right) \, d\mathbf{x} + F_1,$$

where F_1 is the low-order term, and the first term on right-hand side is sign-preserved due to the uniform coerciveness of \mathbf{a}^ε in Assumption (I). As for \mathcal{J}_2 , applying (C.3) with $\mathbf{v} = a_{ij}^\varepsilon \partial_j \mathcal{H}_e^\varepsilon(\mathbf{m}^\varepsilon)$, it leads to

$$\begin{aligned}
\text{(C.12)} \quad \mathcal{J}_2 & = \sum_{i,j=1}^n \int_{\Omega} \mathbf{m}^\varepsilon \times \left(\frac{\partial}{\partial x_i} \mathbf{m}^\varepsilon \times \mathcal{H}_e^\varepsilon(\mathbf{m}^\varepsilon, U^\varepsilon) \right) \cdot \left(\mathbf{m}^\varepsilon \times a_{ij}^\varepsilon \frac{\partial}{\partial x_j} \mathcal{H}_e^\varepsilon(\mathbf{m}^\varepsilon, U^\varepsilon) \right) \, d\mathbf{x} \\
& - \sum_{i,j=1}^n \int_{\Omega} \left(\mathbf{m}^\varepsilon \times \mathcal{H}_e^\varepsilon(\mathbf{m}^\varepsilon, U^\varepsilon) \cdot \frac{\partial}{\partial x_i} \mathbf{m}^\varepsilon \right) \mathbf{m}^\varepsilon \cdot a_{ij}^\varepsilon \frac{\partial}{\partial x_j} \mathcal{H}_e^\varepsilon(\mathbf{m}^\varepsilon, U^\varepsilon) \, d\mathbf{x}.
\end{aligned}$$

Applying the vector triple product formula (2.33) to the first term, and performing integration by parts on the second term, (C.12) becomes

$$\begin{aligned}
\mathcal{J}_2 & = 2 \sum_{i,j=1}^n \int_{\Omega} (\mathbf{m}^\varepsilon \cdot \mathcal{H}_e^\varepsilon(\mathbf{m}^\varepsilon, U^\varepsilon)) \left(\mathbf{m}^\varepsilon \times a_{ij}^\varepsilon \frac{\partial}{\partial x_j} \mathcal{H}_e^\varepsilon(\mathbf{m}^\varepsilon, U^\varepsilon) \cdot \frac{\partial}{\partial x_i} \mathbf{m}^\varepsilon \right) \, d\mathbf{x} + F_2 \\
& \leq C \|\nabla \mathbf{m}^\varepsilon\|_{L^6(\Omega)}^6 + C \|\mathcal{H}_e^\varepsilon(\mathbf{m}^\varepsilon, U^\varepsilon)\|_{L^3(\Omega)}^3 + \delta \|\mathbf{m}^\varepsilon \times \nabla \mathcal{H}_e^\varepsilon(\mathbf{m}^\varepsilon, U^\varepsilon)\|_{L^2(\Omega)}^2 + F_2,
\end{aligned}$$

where F_2 is the low-order term. It can be proved that F_i ($i = 1, 2$) satisfy the following estimate by utilizing (C.2) and Hölder's inequality

$$F_i \leq C + C \|\nabla \mathbf{m}^\varepsilon\|_{L^6(\Omega)}^6 + C \|\mathcal{H}_e^\varepsilon(\mathbf{m}^\varepsilon, U^\varepsilon)\|_{L^3(\Omega)}^3.$$

Substituting the above results into (C.11), applying estimate (C.1) and Lemma C.1, we can finally derive

$$\begin{aligned}
(C.13) \quad & \frac{1}{2} \frac{d}{dt} \|\mathcal{A}_\varepsilon \mathbf{m}^\varepsilon\|_{L^2(\Omega)}^2 + (\alpha a_{\min} - C\delta) \|\mathbf{m}^\varepsilon \times \nabla \mathcal{H}_\varepsilon^\varepsilon(\mathbf{m}^\varepsilon, U^\varepsilon)\|_{L^2(\Omega)}^2 \\
& \leq C + C \|\mathcal{A}_\varepsilon \mathbf{m}^\varepsilon\|_{L^2(\Omega)}^6 + C \|\partial_t \mathbf{m}^\varepsilon\|_{L^2(\Omega)}^2 - \frac{d}{dt} \int_\Omega \mathcal{A}_\varepsilon \mathbf{m}^\varepsilon \cdot \Gamma^\varepsilon(\mathbf{m}^\varepsilon, U^\varepsilon) \, d\mathbf{x}.
\end{aligned}$$

Integrating (C.13) over $[0, t]$ and utilizing (C.10) along with the following inequality

$$\int_\Omega \mathcal{A}_\varepsilon \mathbf{m}^\varepsilon \cdot \Gamma^\varepsilon(\mathbf{m}^\varepsilon, U^\varepsilon) \, d\mathbf{x} \leq C \|\Gamma^\varepsilon(\mathbf{m}^\varepsilon)\|_{L^2(\Omega)}^2 + \frac{1}{4} \|\mathcal{A}_\varepsilon \mathbf{m}^\varepsilon\|_{L^2(\Omega)}^2,$$

it can be proved that for any $t \in (0, T]$

$$(C.14) \quad \frac{1}{4} \|\mathcal{A}_\varepsilon \mathbf{m}^\varepsilon(t)\|_{L^2(\Omega)}^2 \leq C + C \int_0^t \|\mathcal{A}_\varepsilon \mathbf{m}^\varepsilon(\tau)\|_{L^2(\Omega)}^6 \, d\tau,$$

where C depends on $\|\mathcal{A}_\varepsilon \mathbf{m}^\varepsilon(0)\|_{L^2(\Omega)}$, $\mathcal{G}_\varepsilon^\varepsilon[\mathbf{m}^\varepsilon(0), U^\varepsilon(0)]$. With Proposition B.2 and Assumption (II), it can be proved that C is independent of ε and t . Let $F(t)$ denote the right-hand side of (C.14), it follows that

$$\frac{d}{dt} F(t) \leq C F^3(t).$$

By the Cauchy-Lipshitz-Picard Theorem [5] and the comparison principle, there exists $T^* \in (0, T]$ independent of ε , such that $F(t)$ is uniformly bounded on $[0, T^*]$. Thus, $\|\mathcal{A}_\varepsilon \mathbf{m}^\varepsilon(t)\|_{L^2(\Omega)}^2$ is uniformly bounded by (C.14). \square

Finally, Lemma 3.8 can be derived by Lemma C.2. The proof is completed.

REFERENCES

- [1] F. ALOUGES AND G. DI FRATTA, *Homogenization of composite ferromagnetic materials*, Proceedings of the Royal Society A: Mathematical, Physical and Engineering Sciences, 471 (2015), p. 20150365.
- [2] F. ALOUGES AND A. SOYEUR, *On global weak solutions for landau-lifshitz equations: Existence and nonuniqueness*, Nonlinear Analysis: Theory, Methods & Applications, 18 (1992), pp. 1071–1084.
- [3] U. BA AS, M. PAGE, D. PRAETORIUS, AND J. ROCHAT, *A decoupled and unconditionally convergent linear FEM integrator for the Landau-Lifshitz-Gilbert equation with magnetostriction*, IMA Journal of Numerical Analysis, 34 (2014), pp. 1361–1385.
- [4] S. BARTELS AND A. PROHL, *Convergence of an Implicit Finite Element Method for the Landau-Lifshitz-Gilbert Equation*, SIAM Journal on Numerical Analysis, 44 (2006), pp. 1405–1419.
- [5] H. BREZIS AND H. BRÉZIS, *Functional analysis, Sobolev spaces and partial differential equations*, vol. 2, Springer, 2011.
- [6] G. CARBOU, M. EFENDIEV, AND P. FABRIE, *Global weak solutions for the landau-lifshitz equation with magnetostriction*, Mathematical methods in the applied sciences, 34 (2011), pp. 1274–1288.
- [7] G. CARBOU AND P. FABRIE, *Regular solutions for Landau-Lifshitz equation in a bounded domain*, Differential and Integral Equations, 14 (2001), pp. 213–229.
- [8] G. CARBOU AND P. FABRIE, *Regular solutions for landau-lifshitz equation in \mathbb{R}^3* , Communications in Applied Analysis, 5 (2001), pp. 17–30.
- [9] J. CHEN, R. DU, Z. MA, Z. SUN, AND L. ZHANG, *On the Multiscale Landau-Lifshitz-Gilbert Equation: Two-Scale Convergence and Stability Analysis*, Multiscale Modeling & Simulation, 20 (2022), pp. 835–856.
- [10] J. CHEN, J.-G. LIU, AND Z. SUN, *Homogenization of the Landau-Lifshitz-Gilbert Equation with Natural Boundary Condition*, arXiv preprint arXiv:2206.10948, (2022).

- [11] C. CHOQUET, M. MOUMNI, AND M. TILIOUA, *Homogenization of the landau-lifshitz-gilbert equation in a contrasted composite medium*, Discrete & Continuous Dynamical Systems-S, 11 (2018), p. 35.
- [12] I. CIMRÁK AND R. VAN KEER, *Higher order regularity results in 3d for the landau-lifshitz equation with an exchange field*, Nonlinear Analysis: Theory, Methods & Applications, 68 (2008), pp. 1316–1331.
- [13] H. DONG, Z. YANG, X. GUAN, AND J. CUI, *Stochastic higher-order three-scale strength prediction model for composite structures with micromechanical analysis*, Journal of Computational Physics, 465 (2022), p. 111352.
- [14] M. FEISCHL AND T. TRAN, *Existence of regular solutions of the landau-lifshitz-gilbert equation in 3d with natural boundary conditions*, SIAM Journal on Mathematical Analysis, 49 (2017), pp. 4470–4490.
- [15] G. GIOIA AND R. D. JAMES, *Micromagnetics of very thin films*, Proceedings of the Royal Society of London. Series A: Mathematical, Physical and Engineering Sciences, 453 (1997), pp. 213–223.
- [16] A. HAMLER, V. GORIČAN, B. ŠUŠTARŠIČ, AND A. SIRC, *The use of soft magnetic composite materials in synchronous electric motor*, Journal of Magnetism and Magnetic Materials, 304 (2006), pp. e816–e819.
- [17] K. JIANG, L. JU, J. LI, AND X. LI, *Unconditionally stable exponential time differencing schemes for the mass-conserving ALLEN – CAHN equation with nonlocal and local effects*, Numerical Methods for Partial Differential Equations, 38 (2022), pp. 1636–1657.
- [18] L. LANDAU AND E. LIFSHITS, *On the theory of the dispersion of magnetic permeability in ferromagnetic bodies*, in Perspectives in Theoretical Physics, vol. 8, Elsevier, 1935, pp. 153–169.
- [19] P. D. LAX AND R. D. RICHTMYER, *Survey of the stability of linear finite difference equations*, Communications on pure and applied mathematics, 9 (1956), pp. 267–293.
- [20] L. LEITENMAIER AND O. RUNBORG, *On homogenization of the landau lifshitz-equation with rapidly oscillating material coefficient*, Communications in Mathematical Sciences, 20 (2022), pp. 653–694.
- [21] L. LEITENMAIER AND O. RUNBORG, *Upscaling errors in heterogeneous multiscale methods for the landau-lifshitz equation*, Multiscale Modeling & Simulation, 20 (2022), pp. 1–35.
- [22] Z. LU AND J. HUANG, *A multiscale asymptotic expansion for combustion system with composite materials*, Journal of Computational and Applied Mathematics, 441 (2024), p. 115678.
- [23] V. MAKHOTKIN, B. SHURUKHIN, V. LOPATIN, P. Y. MARCHUKOV, AND Y. K. LEVIN, *Magnetic field sensors based on amorphous ribbons*, Sensors and Actuators A: Physical, 27 (1991), pp. 759–762.
- [24] D. PRAETORIUS, *Analysis of the operator delta div arising in magnetic models*, Zeitschrift Fur Analysis Und Ihre Anwendungen, 23 (2004), pp. 589–605.
- [25] P. RASAILI, N. K. SHARMA, AND A. BHATTARAI, *Comparison of ferromagnetic materials: Past work, recent trends, and applications*, Condensed Matter, 7 (2022), p. 12.
- [26] K. SANTUGINI-REPIQUET, *Homogenization of the demagnetization field operator in periodically perforated domains*, Journal of mathematical analysis and applications, 334 (2007), pp. 502–516.
- [27] Z. SHEN, *Periodic Homogenization of Elliptic Systems*, vol. 269 of Operator Theory: Advances and Applications, Springer International Publishing, Cham, 2018.
- [28] P. L. SULEM, C. SULEM, AND C. BARDOS, *On the continuous limit for a system of classical spins*, Communications in Mathematical Physics, 107 (1986), pp. 431–454.
- [29] M. VOPSON, E. ZEMAITYTE, M. SPREITZER, AND E. NAMVAR, *Multiferroic composites for magnetic data storage beyond the super-paramagnetic limit*, Journal of Applied Physics, 116 (2014), p. 113910.
- [30] Z. WANG, S. FU, AND E. CHUNG, *Local multiscale model reduction using discontinuous galerkin coupling for elasticity problems*, Computer Methods in Applied Mechanics and Engineering, 403 (2023), p. 115713.
- [31] E. WEINAN AND B. ENGQUIST, *The heterogenous multiscale methods*, Communications in Mathematical Sciences, 1 (2003), pp. 87–132.
- [32] L. YANG, J. CHEN, AND G. HU, *A framework of the finite element solution of the Landau-Lifshitz-Gilbert equation on tetrahedral meshes*, Journal of Computational Physics, 431 (2021), p. 110142.
- [33] C. YE AND E. T. CHUNG, *Constraint energy minimizing generalized multiscale finite element method for inhomogeneous boundary value problems with high contrast coefficients*, Multiscale Modeling & Simulation, 21 (2023), pp. 194–217.